

UNIVERSITÉ DE GENÈVE

SCHOLA GENEVENSIS MDLIX



DEGENERATE BESS MODEL: the possibility of a low energy strong electroweak sector*

R. Casalbuoni^(a,b), A. Deandrea^(c), S. De Curtis^(b)
D. Dominici^(a,b), R. Gatto^(c), M. Grazzini^(d,e)

(a) Dipart. di Fisica, Univ. di Firenze, Largo E. Fermi, 2; I-50125 Firenze

(b) I.N.F.N., Sezione di Firenze, Largo E. Fermi, 2; I-50125 Firenze

(c) Dépt. Phys. Théorique, Univ. de Genève, 24 quai E.-Ansermet, CH-1211 Genève 4

(d) Dipart. di Fisica, Univ. di Parma, Viale delle Scienze; I-43100 Parma

(e) I.N.F.N., Gruppo Collegato Parma, Viale delle Scienze; I-43100 Parma

UGVA-DPT 1995/10-906

hep-ph/9510431

October 1995

* Partially supported by the Swiss National Foundation

ABSTRACT

We discuss possible symmetries of effective theories describing spinless and spin 1 bosons, mainly to concentrate on an intriguing phenomenological possibility: that of a hardly noticeable strong electroweak sector at relatively low energies. Specifically, a model with both vector and axial vector strong interacting bosons may possess a discrete symmetry imposing degeneracy of the two sets of bosons (degenerate BESS model). In such a case its effects at low energies become almost invisible and the model easily passes all low energy precision tests. The reason lies essentially in the fact that the model automatically satisfies decoupling, contrary to models with only vectors. For large mass of the degenerate spin one bosons the model becomes identical at the classical level to the standard model taken in the limit of infinite Higgs mass. For these reasons we have thought it worthwhile to fully develop the model, together with its possible generalizations, and to study the expected phenomenology. For instance, just because of its invisibility at low energy, it is conceivable that degenerate BESS has low mass spin one states and gives quite visible signals at existing or forthcoming accelerators.

1 Introduction

In a first part of this work we shall give a general discussion of possible properties of low-energy effective theories which describe light pseudoscalar mesons, vector and axial vector mesons, as for instance the bosonic sector of low-energy QCD. Indeed QCD itself may be a testing ground for one particular specification among the low energy effective theories to be discussed. However our main interest here will not be QCD, but rather an alternative possible specification of the low energy theory which may be relevant for an effective description of the phenomenology arising from schemes of strong electroweak breaking.

The bulk of this work will be devoted to the formulation of such a highly symmetric form of low energy effective theory and to the derivation of the very remarkable electroweak phenomenology that it would originate. In a simple model one would think of Goldstone bosons absorbed to give masses to W and Z and, besides, vector and axial vector resonances as the most visible manifestations at low energy of the strong interacting sector.

We shall call G the symmetry group of the theory, spontaneously broken, of which the pseudoscalars are the Goldstone bosons. The vector and axial vector mesons will transform under the unbroken subgroup H of G . In the sense of the method used by CCWZ [1] the vector and axial vector mesons can be treated as matter fields.

It will be a formal expedient to consider the new vector and axial vector fields as gauge bosons of a local symmetry H' , which is spontaneously broken. The local symmetry H' is usually referred to as hidden symmetry [2], [3]. The spin-one bosons acquire their mass, in this description, by absorption of the would-be Goldstones related to the spontaneous breaking of H' . Indeed the peculiar feature of this approach is the explicit presence of these modes. The symmetry group gets enlarged to $G' = G \otimes H'$, where G is global and H' local. The diagonal subgroup of $H \otimes H'$ ($H' \supseteq H$), formally isomorphic to H , is called H_D and it is the invariance group of the vacuum.

We shall mainly consider the case $G = SU(2)_L \otimes SU(2)_R$, $H' = SU(2)_L \otimes SU(2)_R$ and $H_D = SU(2)_V$, where H_D is the diagonal $SU(2)$ subgroup of G' . The group G' breaks down spontaneously to H_D and gives rise to nine Goldstones. Of these, six are absorbed by the vector and axial vector bosons, which are triplets of $SU(2)_V$. The three Goldstones remaining in the spectrum are massless, at least as long as a part of G is not promoted to a local group. This situation is discussed in [2] for QCD and in [4] in the context of dynamical electroweak symmetry breaking.

The detailed study of the symmetries of the effective theory shows however that in special cases the resulting symmetry can be larger than the one requested by the construction. For particular choices of the parameters, a maximal symmetry $[SU(2) \otimes SU(2)]^3$ can be realized for the low energy effective lagrangian of the pseudoscalar, vector-, and axial vector- bosons. Two choices are possible. One can be seen as the natural generalization of the vector symmetry of Georgi [5] for the case when axial vector mesons are also included in addition to the vector mesons of the vector-symmetry; this choice has been considered in ref. [6].

The second choice is the one on which we shall focus here. It may be useful in relation to schemes of strong electroweak breaking. In fact it has the interesting feature of allowing

for a low energy strong electroweak resonant sector while satisfying at the same time the severe constraints from low energy experiments, particularly from LEP/SLC. As such it offers possibilities of experimental test even with future or existing machines of relatively low energy. The phenomenological implications will be a substantial part of our discussion below.

The type of realization of the maximal symmetry $[SU(2) \otimes SU(2)]^3$ on which we shall focus in this work automatically implies degenerate vector and axial vector mesons which have the property of not coupling to the pseudoscalars. The model, after introducing the gauge couplings of the electroweak vector bosons, will be called degenerate BESS (BESS stands for Breaking Electroweak Symmetry Strongly). We shall study in detail its phenomenology. We stress immediately its main property and what makes it so attractive: in degenerate BESS, also when extended to a larger initial symmetry (for instance $SU(8)$ in place of $SU(2)$), one generally derives that all deviations in the low energy parameters from their standard model (SM) values are strongly suppressed. This would make it possible that a strong electroweak sector at relatively low energies exists within the precision of electroweak tests, such that it may be accessible with existing accelerators (Tevatron) or with accelerators in construction or projected for the near future. In fact one can show that the lagrangian of degenerate BESS becomes identical to that of the standard model (except for the Higgs sector) for sufficiently large mass of the degenerate vector and axial vector mesons. In other words, different from ordinary BESS [7], where such a high mass decoupling is not satisfied, the decoupling occurs in degenerate BESS.

The decoupling theorem valid for degenerate BESS requires an accurate study of the contributions of momentum dependent terms to virtual effects of the heavy particles. One can then evaluate such virtual effects for LEP and Tevatron, and subsequently examine what modification of the trilinear gauge couplings may be visible at higher energy e^+e^- colliders. The discussion requires careful redefinition of the physical constants in terms of the parameters of the effective lagrangian. As well known, in the low energy limits one can parameterize the modifications due to the heavy sector in terms of three independent parameters (Δr_W , Δk , $\Delta \rho$, or equivalently ϵ_1 , ϵ_2 , ϵ_3). Radiative corrections have also to be taken into account. The result of this analysis, that we shall present first, shows that in degenerate BESS relatively light resonances are indeed compatible with the electroweak data, as given by LEP and Tevatron.

Besides studying the virtual effects of the heavy resonances we shall also discuss their direct production. To this aim full couplings to fermions and the trilinear couplings among the physical bosons are needed; physical quantities must be carefully identified by renormalizing the occurring expressions and choosing the electric charge, the Z mass, and the Fermi constant as physical inputs. Our phenomenological applications include discussion of the properties of the heavy resonances (masses, partial widths) and studies of their effects at Tevatron, at e^+e^- colliders, and at hadron colliders. The Tevatron limits on W' can be used to limit the parameter space of degenerate BESS. A feature of degenerate BESS, as compared to BESS with only vector resonances, comes from the absence of direct coupling of the new resonances to the longitudinal weak gauge bosons. This implies larger widths into fermion pairs as compared to widths into pairs of weak gauge bosons. Comparison of the limits one can get from CDF to those from LEP shows that CDF is more efficient in limiting low resonance masses while LEP is more efficient for larger masses.

The sensitivity of degenerate BESS at LEP2 and higher energy linear colliders will be discussed by comparing cross-sections and asymmetries in the fermionic pair channels

and WW channel between the model and SM. For LEP2 the general conclusion will be that the bounds on the model would not be much stronger than those from LEP. Substantial improvements are expected from a 500 GeV e^+e^- collider for 20 fb^{-1} , even without beam polarization. The WW final state does not contribute in an important way to the attainable bounds which come essentially from the fermion channels alone (this is a characteristic of degenerate BESS, as already said). Hadron colliders would be complementary to e^+e^- colliders and hopefully will allow for direct study of the new resonant states. For instance, a charged resonance with mass of 500 GeV could give at LHC a spectacular signal. Higher masses up to 1.5 TeV would still give significant signals. Degenerate BESS would thus be comparatively much more evident than ordinary BESS, and probably than any other strong electroweak model not sharing its peculiar symmetry properties.

In section 2 we recall briefly the effective lagrangian formalism we employ in describing vector and axial vector resonances. In section 3 we introduce the lagrangian describing our model with extended symmetry of degenerate vector and axial vector resonances. In sections 4, 5, 6 and 7 we consider the low energy limit of the model, integrating out the new vector and axial vector bosons, both considering the leading order and the next-to-leading order. Implications for the LEP observables are derived as well as other virtual effects of the heavy particles that may be relevant at low energy. In sections 8, 9 and 10 we consider the possibility of direct production of the heavy resonances, so the predictions of the complete lagrangian of the theory are derived, such as mass formulae and eigenstates of the new particles, fermionic and trilinear couplings. In section 11 the physical quantities of the model are identified with the usual renormalization procedures. In section 12 width formulae of relevance in the study of the model are derived. In sections 13, 14 and 15 we discuss the phenomenological implications of the model at present and future high energy accelerators.

2 Extended Vector-Axial Symmetry

Let us consider the following group structure: $G = SU(2)_L \otimes SU(2)_R$, $H' = SU(2)_L \otimes SU(2)_R$ and $H_D = SU(2)_V$, as already stated in the introduction. The nine Goldstone bosons resulting from the spontaneous breaking of $G' = G \otimes H'$ to H_D , can be described by three independent $SU(2)$ elements: L , R and M , transforming with respect to G and H' as follows

$$L' = g_L L h_L, \quad R' = g_R R h_R, \quad M' = h_R^\dagger M h_L \quad (2.1)$$

with $g_{L,R} \in G$ and $h_{L,R} \in H'$. Moreover we shall require the invariance under the discrete left-right transformation, denoted by P

$$P : \quad L \leftrightarrow R, \quad M \leftrightarrow M^\dagger \quad (2.2)$$

which ensures that the low energy theory is parity conserving.

If we ignore the transformations of eq. (2.1), the largest possible global symmetry of the low energy theory is given by the requirement of maintaining for the transformed variables L' , R' and M' , the character of $SU(2)$ elements.

The maximal symmetry is given by the group $G_{max} = [SU(2) \otimes SU(2)]^3$, consisting of three independent $SU(2) \otimes SU(2)$ factors, acting on each of the three variables separately.

It happens that, for specific choices of the parameters of the theory, the symmetry G' gets enlarged to G_{max} .

The most general $G' \otimes P$ invariant lagrangian is given by [4]

$$\mathcal{L}_G = -\frac{v^2}{4}[a_1 I_1 + a_2 I_2 + a_3 I_3 + a_4 I_4] \quad (2.3)$$

plus the kinetic terms \mathcal{L}_{kin} . The terms I_i ($i = 1, \dots, 4$) are given by:

$$\begin{aligned} I_1 &= tr[(V_0 - V_1 - V_2)^2] \\ I_2 &= tr[(V_0 + V_2)^2] \\ I_3 &= tr[(V_0 - V_2)^2] \\ I_4 &= tr[V_1^2] \end{aligned} \quad (2.4)$$

and

$$\begin{aligned} V_0^\mu &= L^\dagger D^\mu L \\ V_1^\mu &= M^\dagger D^\mu M \\ V_2^\mu &= M^\dagger (R^\dagger D^\mu R) M \end{aligned} \quad (2.5)$$

The covariant derivatives are

$$\begin{aligned} D_\mu L &= \partial_\mu L - L \mathbf{L}_\mu \\ D_\mu R &= \partial_\mu R - R \mathbf{R}_\mu \\ D_\mu M &= \partial_\mu M - M \mathbf{L}_\mu + \mathbf{R}_\mu M \end{aligned} \quad (2.6)$$

The kinetic term is

$$\mathcal{L}_{kin} = \frac{1}{g''^2} tr[F_{\mu\nu}(\mathbf{L})]^2 + \frac{1}{g''^2} tr[F_{\mu\nu}(\mathbf{R})]^2 \quad (2.7)$$

where g'' is the gauge coupling constant for the gauge fields \mathbf{L}_μ and \mathbf{R}_μ ,

$$F_{\mu\nu}(\mathbf{L}) = \partial_\mu \mathbf{L}_\nu - \partial_\nu \mathbf{L}_\mu + [\mathbf{L}_\mu, \mathbf{L}_\nu] \quad (2.8)$$

and the same definition holds for $F_{\mu\nu}(\mathbf{R})$. In eq. (2.3) v represents a physical scale related to the spontaneous symmetry breaking of the theory, depending on the particular context under investigation.

The quantities V_i^μ ($i = 0, 1, 2$) are invariant under the global symmetry G and covariant under the gauge group H'

$$(V_i^\mu)' = h_L^\dagger V_i^\mu h_L \quad (2.9)$$

Using the V_i^μ one can build six independent quadratic invariants, which reduce to the four I_i listed above, when parity conservation is required.

For generic values of the parameters a_1 , a_2 , a_3 , a_4 , the lagrangian \mathcal{L} is invariant under $G' \otimes P = G \otimes H' \otimes P$. There are however special choices which enhance the symmetry group [6].

The case of interest for the electroweak sector is provided by the choice: $a_4 = 0$, $a_2 = a_3$. In order to discuss the symmetry properties it is useful to observe that the invariant I_1 can be re-written as follows

$$I_1 = -tr(\partial_\mu U^\dagger \partial^\mu U) \quad (2.10)$$

with

$$U = LM^\dagger R^\dagger \quad (2.11)$$

and the lagrangian becomes

$$\mathcal{L}_G = \frac{v^2}{4} \{a_1 \text{tr}(\partial_\mu U^\dagger \partial^\mu U) + 2 a_2 [\text{tr}(D_\mu L^\dagger D^\mu L) + \text{tr}(D_\mu R^\dagger D^\mu R)]\} \quad (2.12)$$

Each of the three terms in the above expression is invariant under an independent $SU(2) \otimes SU(2)$ group

$$U' = \omega_L U \omega_R^\dagger, \quad L' = g_L L h_L, \quad R' = g_R R h_R \quad (2.13)$$

Moreover, whereas these transformations act globally on the U fields, for the variables L and R , an $SU(2)$ subgroup is local. The overall symmetry is $G_{max} = [SU(2) \otimes SU(2)]^3$, with a part H' realized as a gauge symmetry.

The field redefinition from the variables L , R and M to L , R and U has no effect on the physical content of the theory.

The extra symmetry related to the independent transformation over the U field, can also be expressed in terms of the original variable M . Indeed the lagrangian of eq. (2.3), for $a_4 = 0$, $a_2 = a_3$, possesses the additional invariance

$$L' = L, \quad R' = R, \quad M' = \Omega_R M \Omega_L^\dagger \quad (2.14)$$

with

$$\Omega_L = L^\dagger \omega_L L, \quad \Omega_R = R^\dagger \omega_R R \quad (2.15)$$

By expanding the lagrangian in eq. (2.3) in powers of the Goldstone bosons one finds, as the lowest order contribution, the mass terms for the vector and axial vector mesons

$$\mathcal{L}_G = -\frac{v^2}{4} [a_2 \text{tr}(\mathbf{L}_\mu + \mathbf{R}_\mu)^2 + a_2 \text{tr}(\mathbf{L}_\mu - \mathbf{R}_\mu)^2] + \dots \quad (2.16)$$

where the dots stand for terms at least linear in the Goldstone modes. The mixing between \mathbf{L}_μ and \mathbf{R}_μ is vanishing, and the states are degenerate in mass. Therefore, in the following we will not work with vector and axial vector combinations but with the \mathbf{L}_μ and \mathbf{R}_μ components. Moreover, as it follows from eq. (2.12), the longitudinal modes of the \mathbf{L}_μ and \mathbf{R}_μ fields are entirely provided by the would-be Goldstone bosons in L and R . This means that the pseudoscalar particles remaining as physical states in the low energy spectrum are those associated to U . They in turn can provide the longitudinal components to the W and Z particles, in an effective description of the electroweak breaking sector.

3 The degenerate BESS model

We now consider the coupling of the model to the electroweak $SU(2)_L \otimes U(1)_Y$ gauge fields via the minimal substitution

$$\begin{aligned} D_\mu L &\rightarrow D_\mu L + \tilde{\mathbf{W}}_\mu L \\ D_\mu R &\rightarrow D_\mu R + \tilde{\mathbf{Y}}_\mu R \\ D_\mu M &\rightarrow D_\mu M \end{aligned} \quad (3.1)$$

where

$$\begin{aligned}
\tilde{\mathbf{W}}_\mu &= i\tilde{g}\tilde{W}_\mu^a\frac{\tau^a}{2} \\
\tilde{\mathbf{Y}}_\mu &= i\tilde{g}'\tilde{Y}_\mu\frac{\tau^3}{2} \\
\mathbf{L}_\mu &= i\frac{g''}{\sqrt{2}}L_\mu^a\frac{\tau^a}{2} \\
\mathbf{R}_\mu &= i\frac{g''}{\sqrt{2}}R_\mu^a\frac{\tau^a}{2}
\end{aligned} \tag{3.2}$$

with \tilde{g}, \tilde{g}' the $SU(2)_L \otimes U(1)_Y$ gauge coupling constant and τ^a the Pauli matrices.

By introducing the canonical kinetic terms for W_μ^a and Y_μ we get

$$\mathcal{L} = -\frac{v^2}{4} \left[a_1 \text{tr}(\tilde{\mathbf{W}}_\mu - \tilde{\mathbf{Y}}_\mu)^2 + 2a_2 \text{tr}(\tilde{\mathbf{W}}_\mu - \mathbf{L}_\mu)^2 + 2a_2 \text{tr}(\tilde{\mathbf{Y}}_\mu - \mathbf{R}_\mu)^2 \right] + \mathcal{L}^{kin}(\tilde{\mathbf{W}}, \tilde{\mathbf{Y}}, \mathbf{L}, \mathbf{R}) \tag{3.3}$$

$$\begin{aligned}
\mathcal{L}^{kin}(\tilde{\mathbf{W}}, \tilde{\mathbf{Y}}, \mathbf{L}, \mathbf{R}) &= \frac{1}{2\tilde{g}^2} \text{tr}[F^{\mu\nu}(\tilde{\mathbf{W}})F_{\mu\nu}(\tilde{\mathbf{W}})] + \frac{1}{2\tilde{g}'^2} \text{tr}[F^{\mu\nu}(\tilde{\mathbf{Y}})F_{\mu\nu}(\tilde{\mathbf{Y}})] \\
&+ \frac{1}{g''^2} \text{tr}[F^{\mu\nu}(\mathbf{L})F_{\mu\nu}(\mathbf{L})] + \frac{1}{g''^2} \text{tr}[F^{\mu\nu}(\mathbf{R})F_{\mu\nu}(\mathbf{R})]
\end{aligned} \tag{3.4}$$

We have used tilded quantities to remember that, due to the effects of the \mathbf{L} and \mathbf{R} particles, they are not the physical parameters and fields. In the next sections we will derive the relations between the tilded quantities and the physical ones.

It is natural to think about the model we are considering as a perturbation around the SM picture. The SM relations are obtained in the limit $g'' \gg \tilde{g}, \tilde{g}'$. Actually, for a very large g'' , the kinetic terms for the fields \mathbf{L}_μ and \mathbf{R}_μ drop out, and \mathcal{L} reduces to the first term in eq. (3.3). This term reproduces precisely the mass term for the ordinary gauge vector bosons in the SM, provided we identify the combination $v^2 a_1$ with $1/(\sqrt{2}G_F)$, G_F being the Fermi constant. Therefore in the following we will assume [4]

$$a_1 = 1 \tag{3.5}$$

Finally let us consider the fermions of the SM and denote them by ψ_L and ψ_R . They couple to \mathbf{L} and \mathbf{R} via the mixing with the standard $\tilde{\mathbf{W}}$ and $\tilde{\mathbf{Y}}$:

$$\begin{aligned}
\mathcal{L}_{fermion} &= \bar{\psi}_L i\gamma^\mu \left(\partial_\mu + \tilde{\mathbf{W}}_\mu + \frac{i}{2}\tilde{g}'(B-L)\tilde{Y}_\mu \right) \psi_L \\
&+ \bar{\psi}_R i\gamma^\mu \left(\partial_\mu + \tilde{\mathbf{Y}}_\mu + \frac{i}{2}\tilde{g}'(B-L)\tilde{Y}_\mu \right) \psi_R
\end{aligned} \tag{3.6}$$

where $B(L)$ is the baryon (lepton) number, and

$$\psi = \begin{pmatrix} \psi_u \\ \psi_d \end{pmatrix} \tag{3.7}$$

In addition, we also expect direct couplings to the new vector bosons since they are allowed by the symmetries of \mathcal{L} [7], but, for simplicity, this possibility will not be considered here.

4 The low energy limit

We want to study the effects of the **L** and **R** particles in the low energy limit [8]. This can be done by eliminating the **L** and **R** fields with the solution of their equations of motion for $M_{L,R} \rightarrow \infty$. In fact in this limit the kinetic terms of the new resonances are negligible. Neglecting electromagnetic corrections the common mass of the resonances is given by $M^2 \simeq a_2(v^2/4)g''^2$.

The $M \rightarrow \infty$ limit can be taken in two different ways (we consider v fixed to its experimental value): by sending $g'' \rightarrow \infty$ with a_2 fixed or by fixing g'' and sending $a_2 \rightarrow \infty$. In the first case the **L** and **R** bosons trivially decouple. We will now show that also in the second case we have decoupling due to the extended symmetry $[SU(2) \otimes SU(2)]^3$.

Let us solve the equations of motion for **L** and **R** in this limit. We get

$$\begin{aligned}\mathbf{L}_\mu &= \tilde{\mathbf{W}}_\mu \\ \mathbf{R}_\mu &= \tilde{\mathbf{Y}}_\mu,\end{aligned}\tag{4.1}$$

where the last equation means that only the third isospin component of **R** is different from zero. By substituting these equations in the total lagrangian (see eqs. (3.3) and (3.6) for the case of $SU(2)$) we get

$$\begin{aligned}\mathcal{L}_{eff} &= -\frac{v^2}{4}\text{tr}(\tilde{\mathbf{W}}_\mu - \tilde{\mathbf{Y}}_\mu)^2 \\ &+ \frac{1}{2\tilde{g}^2}\text{tr}[F^{\mu\nu}(\tilde{\mathbf{W}})F_{\mu\nu}(\tilde{\mathbf{W}})] + \frac{1}{2\tilde{g}'^2}\text{tr}[F^{\mu\nu}(\tilde{\mathbf{Y}})F_{\mu\nu}(\tilde{\mathbf{Y}})] \\ &+ \frac{1}{g''^2}\text{tr}[F^{\mu\nu}(\tilde{\mathbf{W}})F_{\mu\nu}(\tilde{\mathbf{W}})] + \frac{1}{g''^2}\text{tr}[F^{\mu\nu}(\tilde{\mathbf{Y}})F_{\mu\nu}(\tilde{\mathbf{Y}})] \\ &+ \mathcal{L}_{fermion}\end{aligned}\tag{4.2}$$

From eq. (4.2) we see that the effective contribution of the **L** and **R** particles give additional terms to the kinetic terms of the standard $\tilde{\mathbf{W}}$ and $\tilde{\mathbf{Y}}$. By the following redefinition of the coupling constants

$$\begin{aligned}\frac{1}{2g^2} &= \frac{1}{2\tilde{g}^2} + \frac{1}{g''^2} \\ \frac{1}{2g'^2} &= \frac{1}{2\tilde{g}'^2} + \frac{1}{g''^2}\end{aligned}\tag{4.3}$$

the effective lagrangian becomes identical to the one of the SM (except for the Higgs sector) showing the decoupling of the theory in the limit $M \rightarrow \infty$. Let us comment about this fact. If one starts from the most general lagrangian, eq. (2.3), gauged according to eq. (3.1), in the limit $M \rightarrow \infty$ the solutions of the equations of motion for **L** and **R** are the following

$$\begin{aligned}\mathbf{L}_\mu &= \frac{1}{2}(1+z)\tilde{\mathbf{W}}_\mu + \frac{1}{2}(1-z)\tilde{\mathbf{Y}}_\mu \\ \mathbf{R}_\mu &= \frac{1}{2}(1-z)\tilde{\mathbf{W}}_\mu + \frac{1}{2}(1+z)\tilde{\mathbf{Y}}_\mu\end{aligned}\tag{4.4}$$

with

$$z = \frac{a_3}{a_3 + a_4}\tag{4.5}$$

By substituting in the lagrangian

$$\begin{aligned}
\mathcal{L}_{eff} &= -\frac{v^2}{4}\text{tr}(\tilde{\mathbf{W}}_\mu - \tilde{\mathbf{Y}}_\mu)^2 \\
&+ \left(\frac{1}{2\tilde{g}^2} + \frac{1}{2g''^2}(1+z^2)\right)\text{tr}[F^{\mu\nu}(\tilde{\mathbf{W}})F_{\mu\nu}(\tilde{\mathbf{W}})] \\
&+ \left(\frac{1}{2\tilde{g}^2} + \frac{1}{2g''^2}(1+z^2)\right)\text{tr}[F^{\mu\nu}(\tilde{\mathbf{Y}})F_{\mu\nu}(\tilde{\mathbf{Y}})] \\
&+ \frac{1}{g''^2}(1-z^2)\text{tr}[F^{\mu\nu}(\tilde{\mathbf{Y}})F_{\mu\nu}(\tilde{\mathbf{W}})] \\
&+ \mathcal{L}_{fermion}
\end{aligned} \tag{4.6}$$

We see that all the corrections to the SM lagrangian depend on the value of the parameter z . In the case we are considering, $a_4 = 0$, $a_2 = a_3$, we have $z = 1$, so the corrections vanish. Notice that the requirement $z = 1$ implies only $a_4 = 0$, so the corrections would be zero also for $a_2 \neq a_3$, but in this case we would not have an enlargement of the symmetry and correspondingly there would be no protection from radiative corrections. The corrections would vanish also for $z = -1$ but again this case does not correspond to an extra-symmetry.

We note that the decoupling remains also valid in the general case of an extended symmetry $[SU(N) \otimes SU(N)]^3$ provided of a suitable redefinition of the $SU(2)_L \otimes U(1)_Y$ gauge coupling constants. When $SU(N) \otimes SU(N) \supset SU(3)$ and one considers also the $SU(3)_{color}$ gauging, a redefinition of the strong gauge coupling constant g_s is necessary as well. This happens for instance in the model considered in ref. [9]. In the case of an extended symmetry $[SU(8) \otimes SU(8)]^3$ we find

$$\begin{aligned}
\frac{1}{2g^2} &= \frac{1}{2\tilde{g}^2} + \frac{1}{g''^2} \\
\frac{1}{2g'^2} &= \frac{1}{2\tilde{g}^2} + \frac{5}{3} \frac{1}{g''^2} \\
\frac{1}{4g_s^2} &= \frac{1}{4\tilde{g}_s^2} + \frac{1}{2g''^2}
\end{aligned} \tag{4.7}$$

5 The low energy limit, next-to-leading order

Since the degenerate BESS model is indistinguishable from the SM at the leading order in the low energy limit ($M \rightarrow \infty$) let us consider the solution of the classical equations of motion for the \mathbf{L} and \mathbf{R} fields by retaining also terms of the order q^2/M^2 . As in sect. 4 we will eliminate the \mathbf{L} and \mathbf{R} fields with the solutions of their equations of motion and we will consider the virtual effects of the heavy particles. We will study the effective theory by considering the limit $g'' \rightarrow \infty$ with corrections up to order $(1/g'')^2$.

Let us solve the equations of motion for \mathbf{L} and \mathbf{R} in this limit. We get

$$\begin{aligned}
\mathbf{L}_\nu &= \left(1 - \frac{\square}{M^2}\right) \tilde{\mathbf{W}}_\nu + \Delta\mathbf{L}_\nu \\
\mathbf{R}_\nu &= \left(1 - \frac{\square}{M^2}\right) \tilde{\mathbf{Y}}_\nu + \Delta\mathbf{R}_\nu
\end{aligned} \tag{5.1}$$

with

$$\begin{aligned}\Delta\mathbf{L}^\nu &= \frac{1}{M^2}\left(\partial^\nu\partial_\mu\tilde{\mathbf{W}}^\mu - \partial_\mu[\tilde{\mathbf{W}}^\mu, \tilde{\mathbf{W}}^\nu] - [\tilde{\mathbf{W}}_\mu, F^{\mu\nu}(\tilde{\mathbf{W}})]\right) \\ \Delta\mathbf{R}^\nu &= \frac{1}{M^2}\left(\partial^\nu\partial_\mu\tilde{\mathbf{Y}}^\mu\right)\end{aligned}\quad (5.2)$$

where the equation for \mathbf{R} means that only the third isospin component of the field is different from zero. $\Delta\mathbf{L}_\mu$ and $\Delta\mathbf{R}_\mu$ contain linear terms proportional to the divergences of the fields and $\Delta\mathbf{L}_\mu$ contains also bilinear and trilinear terms which do not affect the self-energies and contribute to the anomalous trilinear and quadrilinear couplings.

We will examine the virtual effects of the \mathbf{L} and \mathbf{R} fields on the observables. In particular, in the next section, we will focus on the physics at LEP and Tevatron, for which the modifications due to the heavy particles affect the self-energies only. After we will discuss the modifications in the trilinear gauge couplings which will be studied at future e^+e^- colliders.

To discuss the LEP physics we neglect $\Delta\mathbf{L}_\mu$ and $\Delta\mathbf{R}_\mu$ in the solutions (5.1). By substituting in the lagrangian (3.3) we get for the bilinear part (neglecting again divergences of the vector fields)

$$\begin{aligned}\mathcal{L}_{eff}^{(2)} &= -\frac{1}{4}(1+z_\gamma)\tilde{A}_{\mu\nu}\tilde{A}^{\mu\nu} - \frac{1}{2}(1+z_w)\tilde{W}_{\mu\nu}^+\tilde{W}^{\mu\nu-} - \frac{1}{4}(1+z_z)\tilde{Z}_{\mu\nu}\tilde{Z}^{\mu\nu} \\ &+ \frac{1}{2}z_{z\gamma}\tilde{A}_{\mu\nu}\tilde{Z}^{\mu\nu} + \tilde{M}_W^2\tilde{W}^{\mu+}\tilde{W}_\mu^- + \frac{1}{2}\tilde{M}_Z^2\tilde{Z}^\mu\tilde{Z}_\mu \\ &+ \frac{1}{2M^2}\left[\frac{z_z}{2}\tilde{Z}_{\mu\nu}\square\tilde{Z}^{\mu\nu} + \frac{z_\gamma}{2}\tilde{A}_{\mu\nu}\square\tilde{A}^{\mu\nu} - z_{z\gamma}\tilde{Z}_{\mu\nu}\square\tilde{A}^{\mu\nu} + z_w\tilde{W}_{\mu\nu}^+\square\tilde{W}^{-\mu\nu}\right]\end{aligned}\quad (5.3)$$

where

$$\begin{aligned}\tilde{W}_\mu^\pm &= \frac{1}{\sqrt{2}}(\tilde{W}_1 \mp i\tilde{W}_2) \\ \tilde{W}_\mu^3 &= \tilde{s}_\theta\tilde{A}_\mu + \tilde{c}_\theta\tilde{Z}_\mu \\ \tilde{Y}_\mu &= \tilde{c}_\theta\tilde{A}_\mu - \tilde{s}_\theta\tilde{Z}_\mu \\ \tilde{e} &= \tilde{g}\tilde{s}_\theta = \tilde{g}'\tilde{c}_\theta \\ \tilde{M}_W^2 &= \frac{v^2}{4}\tilde{g}^2 \\ \tilde{M}_Z^2 &= \frac{\tilde{M}_W^2}{\tilde{c}_\theta^2}\end{aligned}\quad (5.4)$$

$O_{\mu\nu} = \partial_\mu O_\nu - \partial_\nu O_\mu$, ($O = \tilde{W}^\pm, \tilde{A}, \tilde{Z}$), and

$$z_\gamma = 4s_\theta^2\left(\frac{g}{g''}\right)^2 \quad z_w = 2\left(\frac{g}{g''}\right)^2 \quad z_z = \frac{1+c_{2\theta}^2}{c_\theta^2}\left(\frac{g}{g''}\right)^2 \quad z_{z\gamma} = -2\frac{s_\theta}{c_\theta}c_{2\theta}\left(\frac{g}{g''}\right)^2 \quad (5.5)$$

Notice that $\tilde{g}, \tilde{g}', \tilde{e}, \tilde{s}_\theta, \tilde{c}_\theta$ have the same definitions as in the SM. As stated before, due to the effects of the \mathbf{L} and \mathbf{R} particles, these are not the physical quantities in our model. In eq. (5.5) we have not used the tilded quantities since these parameters are already of the order of $(1/g'')^2$.

The corrections to \mathcal{L}_{SM} are $U(1)_{em}$ invariant and produce a wave-function renormalization of $\tilde{A}_\mu, \tilde{Z}_\mu, \tilde{W}_\mu^\pm$ plus a mixing term $\tilde{A}_\mu - \tilde{Z}_\mu$. We will absorb these corrections

by a convenient redefinition of the fields. Actually there are only three renormalization transformations of the fields $\tilde{A}_\mu, \tilde{Z}_\mu, \tilde{W}_\mu^\pm$ without changing the physics. This means that three of the four deviations $z_\gamma, z_w, z_z, z_{z\gamma}$ are non physical.

To identify the physical quantities we define new fields in such a way to have canonical kinetic terms and to cancel the mixing term $\tilde{A}_\mu - \tilde{Z}_\mu$. They are the following:

$$\begin{aligned}\tilde{A}_\mu &= \left(1 - \frac{z_\gamma}{2}\left(1 - \frac{\square}{M^2}\right)\right)A_\mu + z_{z\gamma}\left(1 - \frac{\square}{M^2}\right)Z_\mu \\ \tilde{W}_\mu^\pm &= \left(1 - \frac{z_w}{2}\left(1 + \frac{M_W^2}{M^2} - \frac{\square}{M^2}\right)\right)W_\mu^\pm \\ \tilde{Z}_\mu &= \left(1 - \frac{z_z}{2}\left(1 + \frac{M_Z^2}{M^2} - \frac{\square}{M^2}\right)\right)Z_\mu\end{aligned}\quad (5.6)$$

Working at the first order in $1/M^2$ and in $1/g'^2$, we do not make distinction in the coefficients of these parameters between "tilded" and physical quantities. By substituting in (5.3) we get

$$\begin{aligned}\mathcal{L}_{eff}^{(2)} &= -\frac{1}{4}A_{\mu\nu}A^{\mu\nu} - \frac{1}{2}W_{\mu\nu}^+W^{\mu\nu-} - \frac{1}{4}Z_{\mu\nu}Z^{\mu\nu} \\ &+ \tilde{M}_W^2\left(1 - z_w\left(1 + \frac{M_W^2}{M^2}\right)\right)W^{\mu+}W_\mu^- + \frac{1}{2}\tilde{M}_Z^2\left(1 - z_z\left(1 + \frac{M_Z^2}{M^2}\right)\right)Z^\mu Z_\mu\end{aligned}\quad (5.7)$$

From which we obtain the values of the physical masses

$$\begin{aligned}M_W^2 &= \tilde{M}_W^2\left(1 - z_w\left(1 + \frac{M_W^2}{M^2}\right)\right) \\ M_Z^2 &= \tilde{M}_Z^2\left(1 - z_z\left(1 + \frac{M_Z^2}{M^2}\right)\right)\end{aligned}\quad (5.8)$$

The field renormalization affects also all the couplings of the standard gauge bosons to the fermions. By separating the charged and the neutral fermionic sector and substituting eq. (5.6) in $\mathcal{L}_{fermion}$ given in (3.6) we get

$$\mathcal{L}_{eff}^{charged} = -\frac{\tilde{e}}{\sqrt{2}\tilde{s}_\theta}\bar{\psi}_d\gamma^\mu\frac{1-\gamma_5}{2}\psi_u\left(1 - \frac{z_w}{2}\left(1 + \frac{M_W^2}{M^2} - \frac{\square}{M^2}\right)\right)W_\mu^- + h.c. \quad (5.9)$$

$$\begin{aligned}\mathcal{L}_{eff}^{neutral} &= -\frac{\tilde{e}}{\tilde{s}_\theta\tilde{c}_\theta}\bar{\psi}\gamma^\mu\left[T_L^3\frac{1-\gamma_5}{2}\right. \\ &- Q\tilde{s}_\theta^2\left(1 - \frac{\tilde{c}_\theta}{\tilde{s}_\theta}z_{z\gamma}\left(1 - \frac{\square_Z}{M^2}\right)\right)]\psi\left(1 - \frac{z_z}{2}\left(1 + \frac{M_Z^2}{M^2} - \frac{\square}{M^2}\right)\right)Z_\mu \\ &- \tilde{e}\bar{\psi}\gamma^\mu Q\psi\left(1 - \frac{z_\gamma}{2}\left(1 - \frac{\square}{M^2}\right)\right)A_\mu\end{aligned}\quad (5.10)$$

with the standard definitions:

$$\begin{aligned}Q &= \frac{\tau^3}{2} + \frac{B-L}{2} \\ T_L^3\psi_L &= \frac{\tau^3}{2}\psi_L \quad T_L^3\psi_R = 0\end{aligned}\quad (5.11)$$

and \square_Z operates only on the Z field.

The physical constants as the electric charge, the Fermi constant and the mass of the Z , which are the input parameters for the physics at LEP, must be redefined in terms of

the parameters appearing in our effective lagrangian. The physical mass of the Z is given in eq. (5.8). The physical electric charge is defined at zero momentum, then, from eq. (5.10)

$$e = \tilde{e}\left(1 - \frac{z_\gamma}{2}\right) \quad (5.12)$$

The Fermi constant G_F , is defined from the μ -decay process, again at zero momentum. Since the charged current coupling (see eq. (5.9)) is modified by a factor $(1 - z_w(1 + M_W^2/M^2)/2)$ and the W mass is given in eq. (5.8) we get

$$\frac{G_F}{\sqrt{2}} = \frac{\tilde{e}^2\left(1 - z_w\left(1 + \frac{M_W^2}{M^2}\right)\right)}{8\tilde{s}_\theta^2\tilde{M}_W^2\left(1 - z_w\left(1 + \frac{M_W^2}{M^2}\right)\right)} = \frac{e^2}{8\tilde{s}_\theta^2\tilde{c}_\theta^2 M_Z^2}\left(1 - z_z\left(1 + \frac{M_Z^2}{M^2}\right) + z_\gamma\right) \quad (5.13)$$

where in the second equality we have used eqs. (5.4), (5.8) and (5.12). Finally, we define s_θ and c_θ by equating the last expression to the one in the SM (tree level): $G_F/\sqrt{2} = e^2/(8s_\theta^2c_\theta^2M_Z^2)$. We get

$$s_\theta^2c_\theta^2 = \tilde{s}_\theta^2\tilde{c}_\theta^2\left(1 + z_z\left(1 + \frac{M_Z^2}{M^2}\right) - z_\gamma\right) \quad (5.14)$$

that is

$$\begin{aligned} s_\theta^2 &= \tilde{s}_\theta^2\left(1 + \frac{c_\theta^2}{c_{2\theta}}\left(z_z\left(1 + \frac{M_Z^2}{M^2}\right) - z_\gamma\right)\right) \\ c_\theta^2 &= \tilde{c}_\theta^2\left(1 - \frac{s_\theta^2}{c_{2\theta}}\left(z_z\left(1 + \frac{M_Z^2}{M^2}\right) - z_\gamma\right)\right) \end{aligned} \quad (5.15)$$

6 Calculation of the ϵ parameters

Let us now discuss how the effects of the \mathbf{L} and \mathbf{R} modify the observables measured at LEP and Tevatron.

Since, in our model, the modifications due to heavy particles are contained in the propagators of the standard gauge bosons (the so-called oblique corrections), we can apply the analysis made in terms of the ϵ parameters [10].

Let us start from the M_W measurement. It is customary to define

$$\frac{M_W^2}{M_Z^2} = c_\theta^2\left[1 - \frac{s_\theta^2}{c_{2\theta}}\Delta r_W\right] \quad (6.1)$$

From the relation $\tilde{M}_W^2 = \tilde{M}_Z^2\tilde{c}_\theta^2$ we get

$$\frac{M_W^2}{M_Z^2} = c_\theta^2\left[1 + z_z\left(1 + \frac{M_Z^2}{M^2}\right) - z_w\left(1 + \frac{M_W^2}{M^2}\right) - \frac{s_\theta^2}{c_{2\theta}}\left(z_\gamma - z_z\left(1 + \frac{M_Z^2}{M^2}\right)\right)\right] \quad (6.2)$$

so, for comparison

$$\Delta r_W = z_\gamma + \frac{c_{2\theta}}{s_\theta^2}z_w\left(1 + \frac{M_W^2}{M^2}\right) - \frac{c_\theta^2}{s_\theta^2}z_z\left(1 + \frac{M_Z^2}{M^2}\right) = -X \quad (6.3)$$

where in the second equality we have used eq. (5.5) and

$$X = 2 \frac{M_Z^2}{M^2} \left(\frac{g}{g''} \right)^2 \quad (6.4)$$

The neutral current couplings to the Z are defined by

$$\mathcal{L}^{neutral}(Z) = -\frac{e}{s_\theta c_\theta} \left(1 + \frac{\Delta\rho}{2} \right) Z_\mu \bar{\psi} [\gamma^\mu g_V + \gamma^\mu \gamma_5 g_A] \psi \quad (6.5)$$

with

$$\begin{aligned} g_V &= \frac{T_L^3}{2} - s_\theta^2 Q \\ g_A &= -\frac{T_L^3}{2} \\ s_\theta^2 &= (1 + \Delta k) s_\theta^2 \end{aligned} \quad (6.6)$$

By using eqs. (5.12) and (5.14) we get

$$\frac{e}{s_\theta c_\theta} = \frac{\tilde{e}}{\tilde{s}_\theta \tilde{c}_\theta} \left(1 - \frac{z_z}{2} \left(1 + \frac{M_Z^2}{M^2} \right) \right) \quad (6.7)$$

For comparison with eq. (5.10), and using eq. (5.5), we obtain

$$\begin{aligned} \Delta\rho &= -z_z \frac{M_Z^2}{M^2} = -\frac{c_\theta^4 + s_\theta^4}{c_\theta^2} X \\ \Delta k &= \frac{c_\theta^2}{c_{2\theta}} \left(z_\gamma - z_z \left(1 + \frac{M_Z^2}{M^2} \right) \right) - \frac{c_\theta}{s_\theta} z_{z\gamma} \left(1 + \frac{M_Z^2}{M^2} \right) = -\frac{2c_\theta^2 s_\theta^2}{c_{2\theta}} X \end{aligned} \quad (6.8)$$

Summarizing, we have the following correspondence between corrections and observables: Δr_W is equivalent to M_W/M_Z which is measured at Tevatron, Δk modifies the vector coupling g_V and $\Delta\rho$ modifies the neutral coupling overall strength. At LEP, Δk can be obtained by measuring the forward-backward asymmetry at the Z peak. Then, having fixed Δk , $\Delta\rho$ can be determined by the leptonic width. All these quantities receive contributions also from weak radiative corrections. In particular they depend quadratically from the top mass which is still affected by a large error. From the point of view of data analysis it turns out to be more convenient to isolate such contribution in $\Delta\rho$ and define two other linear combinations which depend only logarithmically on m_{top} . They are the so-called ϵ parameters [10]

$$\begin{aligned} \epsilon_1 &= \Delta\rho \\ \epsilon_2 &= c_\theta^2 \Delta\rho + \frac{s_\theta^2}{c_{2\theta}} \Delta r_W - 2s_\theta^2 \Delta k \\ \epsilon_3 &= c_\theta^2 \Delta\rho + c_{2\theta} \Delta k \end{aligned} \quad (6.9)$$

Using eqs. (6.3) and (6.8) we get

$$\begin{aligned} \epsilon_1 &= -\frac{c_\theta^4 + s_\theta^4}{c_\theta^2} X \\ \epsilon_2 &= -c_\theta^2 X \\ \epsilon_3 &= -X \end{aligned} \quad (6.10)$$

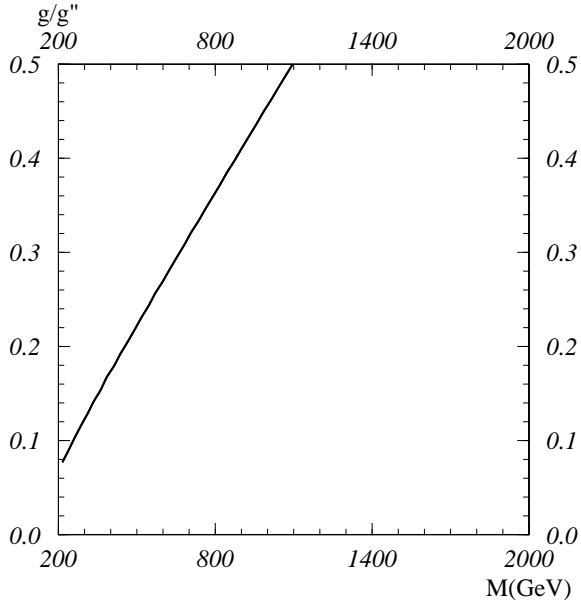


Fig. 1 - 90% C.L. contour on the plane $(M, g/g'')$ obtained by comparing the values of the ϵ parameters from the degenerate BESS model with the experimental data from LEP. The allowed region is below the curve.

All these deviations are of order X which contains a double suppression factor M_Z^2/M^2 and $(g/g'')^2$. These are the same results one obtains from the definitions of the ϵ_i parameters in terms of the self-energies [11], [6]. In the $M \rightarrow \infty$ limit, the model decouples, as already noticed in sect. 6, and the ϵ_i go to zero. The fact that in the degenerate BESS model $\epsilon_3 = 0$ in this limit, follows from the $SU(2)_L \otimes SU(2)_R$ custodial symmetry [12].

The sum of the SM contributions, functions of the top and Higgs masses, and the previous deviations has to be compared with the experimental values for the ϵ parameters, determined from the available LEP data and the M_W measurement from Tevatron [13]

$$\begin{aligned}
 \epsilon_1 &= (3.48 \pm 1.49) \cdot 10^{-3} \\
 \epsilon_2 &= (-5.7 \pm 4.19) \cdot 10^{-3} \\
 \epsilon_3 &= (3.25 \pm 1.40) \cdot 10^{-3}
 \end{aligned}
 \tag{6.11}$$

Taking into account the SM values $(\epsilon_1)_{SM} = 4.4 \cdot 10^{-3}$, $(\epsilon_2)_{SM} = -7.1 \cdot 10^{-3}$, $(\epsilon_3)_{SM} = 6.5 \cdot 10^{-3}$ for $m_{top} = 180 \text{ GeV}$ and $m_H = 1000 \text{ GeV}$, we find, from the combinations of the previous experimental results, the 90% CL limit in the plane $(M, g/g'')$ given in Fig. 1. We see that there is room for relatively light resonances beyond the usual SM spectrum.

7 Anomalous trilinear gauge couplings

Let us evaluate the anomalous contributions to the trilinear gauge couplings at the order q^2/M^2 . As previously observed, since $\Delta \mathbf{R}_\mu$ in eq. (5.2) does not contain bilinear and trilinear terms, the elimination of the \mathbf{R} -field does not give any contribution to the anomalous trilinear and quadrilinear terms.

Substituting the solutions (5.1) in eq. (3.3) we get

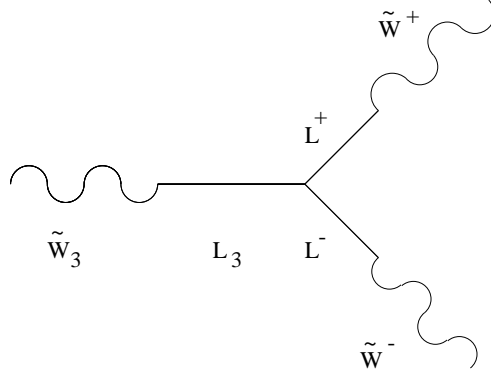


Fig. 2 - Feynman diagram contributing to the anomalous trilinear gauge coupling.

$$\begin{aligned}
\mathcal{L}_{eff}^{kin(3)} &= -i\tilde{g}\{(1+z_w)(\tilde{W}_{\mu\nu}^3 \tilde{W}^{+\mu} \tilde{W}^{-\nu} + \tilde{W}^{3\mu}(\tilde{W}_{\mu\nu}^- \tilde{W}^{+\nu} - \tilde{W}_{\mu\nu}^+ \tilde{W}^{-\nu})) \\
&- \frac{z_w}{M^2}[(\square_3 + \square_- + \square_+)(\tilde{W}_{\mu\nu}^3 \tilde{W}^{+\mu} \tilde{W}^{-\nu} + \tilde{W}^{3\mu}(\tilde{W}_{\mu\nu}^- \tilde{W}^{+\nu} - \tilde{W}_{\mu\nu}^+ \tilde{W}^{-\nu})) \\
&+ ((\partial_\nu \partial^\mu \tilde{W}_\mu^3)(\partial_\rho \tilde{W}^{-\nu}) \tilde{W}^{+\rho} + (\partial_\nu \partial^\mu \tilde{W}_\mu^3)(\partial^\nu \tilde{W}^{+\rho}) \tilde{W}_\rho^- \\
&- (\partial_\nu \partial^\mu \tilde{W}_\mu^-)(\partial_\rho \tilde{W}^{3\nu}) \tilde{W}^{+\rho} + (\partial_\nu \partial^\mu \tilde{W}_\mu^-)(\partial^\nu \tilde{W}^{3\rho}) \tilde{W}_\rho^+ \\
&- (\partial_\nu \partial^\mu \tilde{W}_\mu^-)(\partial^\nu \tilde{W}^{+\rho}) \tilde{W}_\rho^3 + (\partial_\nu \partial^\mu \tilde{W}_\mu^-)(\partial^\rho \tilde{W}^{+\nu}) \tilde{W}_\rho^3 \\
&- \text{h.c.})\} \tag{7.1}
\end{aligned}$$

where we have used the notation \square_a to denote the action of the D'Alembert operator on the fields \tilde{W}^a , and we have freely integrated by parts. This result has been independently checked by evaluating directly the trilinear $\tilde{W}^3 \tilde{W}^+ \tilde{W}^-$ coupling as coming from the mixing $\mathbf{L} - \tilde{\mathbf{W}}$ (see Fig. 2) and expanding the propagators of the \mathbf{L} fields up to the order q^2/M^2 .

The physical vertices are obviously obtained by substituting to \tilde{W}^3 its expression in terms of the photon and the Z fields and by performing fields and couplings renormalization according to section 5.

Since the physical process which is relevant for studying the trilinear gauge couplings is $e^+e^- \rightarrow W^+W^-$, we have

$$\partial_\mu W^{\pm\mu} = 0 \tag{7.2}$$

because the final W 's are on-shell. Also

$$\partial_\mu Z^\mu \simeq \partial_\mu A^\mu \simeq 0 \tag{7.3}$$

because the Z and the photon are coupled to light fermions. Therefore we can neglect all the divergences of the fields in eq. (7.1) and we get

$$\begin{aligned}
\mathcal{L}_{eff}^{kin(3)} &= i\text{ectg}\theta(1 + \frac{z_z}{2c_{2\theta}} \frac{M_Z^2}{M^2} - \frac{z_w}{2} \frac{\square_+ + M_W^2}{M^2} - \frac{z_w}{2} \frac{\square_- + M_W^2}{M^2} - \frac{z_z}{2} \frac{\square_Z + M_Z^2}{M^2}) \\
&\quad (Z^{\mu\nu} W_\mu^- W_\nu^+ + Z^\nu(W_{\mu\nu}^- W^{\mu+} - W_{\mu\nu}^+ W^{\mu-})) \\
&+ ie(1 - \frac{z_w}{2} \frac{\square_+ + M_W^2}{M^2} - \frac{z_w}{2} \frac{\square_- + M_W^2}{M^2} + (\frac{z_\gamma}{2} - z_w) \frac{\square_A}{M^2}) \\
&\quad (A^{\mu\nu} W_\mu^- W_\nu^+ + A^\nu(W_{\mu\nu}^- W^{\mu+} - W_{\mu\nu}^+ W^{\mu-})) \tag{7.4}
\end{aligned}$$

We see that the tensor structure of this correction is the same of the trilinear couplings in the SM.

In the study of the reaction $e^+e^- \rightarrow W^+W^-$ at linear colliders, the structure of the corrections is of the form $(A + B/M^2 s)$, that is we have non trivial form factors [14]. However, notice that the electric charge of the W 's as measured by the coupling with the photon, turns out to be correct, being defined at zero transferred momentum and with the W 's on shell.

8 Masses and eigenstates of spin-1 bosons

Up to now we have been interested in the virtual effects only. In the following we will consider also the possibility of producing directly the heavy resonances. Therefore we need to keep explicitly the corresponding fields in the formalism.

By writing the quadratic part of \mathcal{L} , given in eq. (3.3), in terms of the charged and the neutral fields one finds:

$$\begin{aligned} \mathcal{L}^{(2)} = & \frac{v^2}{4}[(1 + 2a_2)\tilde{g}^2\tilde{W}_\mu^+\tilde{W}^{\mu-} + a_2g''^2(\tilde{L}_\mu^+\tilde{L}^{\mu-} + \tilde{R}_\mu^+\tilde{R}^{\mu-}) \\ & - \sqrt{2}a_2\tilde{g}g''(\tilde{W}_\mu^+\tilde{L}^{\mu-} + \tilde{W}_\mu^-\tilde{L}^{\mu+})] \\ & + \frac{v^2}{8}[(1 + 2a_2)(\tilde{g}^2\tilde{W}_3^2 + \tilde{g}'^2\tilde{Y}^2) + a_2g''^2(\tilde{L}_3^2 + \tilde{R}_3^2) \\ & - 2\tilde{g}\tilde{g}'\tilde{W}_{3\mu}\tilde{Y}^\mu - 2\sqrt{2}a_2g''(\tilde{g}\tilde{W}_3\tilde{L}_3^\mu + \tilde{g}'\tilde{Y}_\mu\tilde{R}_3^\mu)] \end{aligned} \quad (8.1)$$

The reason to introduce $\tilde{\mathbf{L}}$ and $\tilde{\mathbf{R}}$ is to distinguish them from the mass eigenstates.

In the charged sector the fields R^\pm are unmixed for any value of g'' . Their mass is given by:

$$M_{R^\pm}^2 = \frac{v^2}{4}a_2g''^2 \equiv M^2 \quad (8.2)$$

We will parameterize the model in terms of g'' and M .

The mass matrix in the charged sector (\tilde{W}, \tilde{L}) is

$$M_{charged}^2 = \frac{v^2}{4}\tilde{g}^2 \begin{pmatrix} 1 + 2\frac{x^2}{r} & -\sqrt{2}\frac{x}{r} \\ -\sqrt{2}\frac{x}{r} & \frac{1}{r} \end{pmatrix} \quad (8.3)$$

where

$$x = \frac{\tilde{g}}{g''}, \quad r = \frac{v^2}{4} \frac{\tilde{g}^2}{M^2} \quad (8.4)$$

At the order x^2 the eigenvalues are

$$M_{W^\pm}^2 = \frac{v^2}{4}\tilde{g}^2[1 - 2\frac{x^2}{1-r} + \dots] \quad , \quad M_{L^\pm}^2 = \frac{v^2}{4}\frac{\tilde{g}^2}{r}[1 + 2\frac{x^2}{1-r} + \dots] \quad (8.5)$$

Let us call \mathbf{C} the matrix which transforms the fields appearing in the lagrangian (8.1) into the charged eigenstates. We have

$$\begin{pmatrix} W^\pm \\ L^\pm \end{pmatrix} = \mathbf{C}^{-1} \begin{pmatrix} \tilde{W}^\pm \\ \tilde{L}^\pm \end{pmatrix} = \begin{pmatrix} \cos \phi & \sin \phi \\ -\sin \phi & \cos \phi \end{pmatrix} \begin{pmatrix} \tilde{W}^\pm \\ \tilde{L}^\pm \end{pmatrix} \quad (8.6)$$

where

$$\tan \phi = \frac{k}{1 + \sqrt{1 + k^2}}, \quad k = \frac{2\sqrt{2}x}{1 - r - 2x^2} \quad (8.7)$$

The physical particle L^\pm are a combination of \tilde{L}^\pm and \tilde{W}^\pm , which, for small values of x , and for $M \rightarrow \infty$ ($r \rightarrow 0$), are mainly oriented along the \tilde{L}^\pm direction, as it can be seen from the following relations

$$\begin{aligned} W^\pm &= (1 - x^2) \tilde{W}^\pm + \sqrt{2}x \tilde{L}^\pm \\ L^\pm &= -\sqrt{2}x \tilde{W}^\pm + (1 - x^2) \tilde{L}^\pm \end{aligned} \quad (8.8)$$

In the neutral sector there is, as expected, a strictly massless combination which corresponds to the physical photon associated to the unbroken $U(1)$ gauge group. As already discussed in ref. [4] we perform the substitution

$$\begin{aligned} \hat{W}^3 &= \tilde{c}_\theta \tilde{W}^3 - \tilde{s}_\theta \tilde{Y} \\ \hat{Y} &= \tilde{s}_\theta \tilde{W}^3 + \tilde{c}_\theta \tilde{Y} \end{aligned} \quad (8.9)$$

The neutral part of the lagrangian (8.1) is then given by

$$\begin{aligned} \mathcal{L}_{neutral}^{(2)} &= \frac{v^2}{8} [G^2 \hat{W}_3^2 + a_2 (\frac{\tilde{g}^2 - \tilde{g}'^2}{G} \hat{W}_3 + 2 \frac{\tilde{g}\tilde{g}'}{G} \hat{Y} - \frac{g''}{\sqrt{2}} (\tilde{L}_3 + \tilde{R}_3))^2 \\ &+ a_2 (G \hat{W}_3 - \frac{g''}{\sqrt{2}} (\tilde{L}_3 - \tilde{R}_3))^2] \end{aligned} \quad (8.10)$$

where $G = \sqrt{\tilde{g}^2 + \tilde{g}'^2}$. Inspecting this expression, it is natural to define the new linear combinations

$$\begin{aligned} \gamma &= \hat{Y} \cos \psi + \frac{\tilde{L}_3 + \tilde{R}_3}{\sqrt{2}} \sin \psi \\ \hat{V}_3 &= -\hat{Y} \sin \psi + \frac{\tilde{L}_3 - \tilde{R}_3}{\sqrt{2}} \cos \psi \end{aligned} \quad (8.11)$$

where

$$\tan \psi = 2\tilde{s}_\theta x \quad (8.12)$$

We then finally obtain

$$\begin{aligned} \mathcal{L}_{neutral}^{(2)} &= \frac{v^2}{8} [G^2 \hat{W}_3^2 + \frac{E_V^2}{R_V} (G \hat{W}_3 - \frac{G}{E_V} \hat{V}_3)^2 \\ &+ \frac{E_A^2}{R} (G \hat{W}_3 + \frac{G}{E_A} \hat{A}_3)^2] \end{aligned} \quad (8.13)$$

where

$$\begin{aligned} R &= \frac{r}{\tilde{c}_\theta^2} \\ R_V &= \frac{R}{1 + 4x^2 \tilde{s}_\theta^2} \\ E_A &= \frac{x}{\tilde{c}_\theta} \\ E_V &= \frac{\tilde{c}_{2\theta}}{\tilde{c}_\theta} \frac{x}{\sqrt{1 + 4x^2 \tilde{s}_\theta^2}} \\ \hat{A}_3 &= \frac{\tilde{R}_3 - \tilde{L}_3}{\sqrt{2}} \end{aligned} \quad (8.14)$$

The mass matrix for the neutral case in the basis $(\hat{W}_3, \hat{V}_3, \hat{A}_3)$ is the following

$$M_{neutral}^2 = \frac{v^2}{4} G^2 \begin{pmatrix} 1 + \frac{E_V^2}{R_V} + \frac{E_A^2}{R} & -\frac{E_V}{R_V} & \frac{E_A}{R} \\ -\frac{E_V}{R_V} & \frac{1}{R_V} & 0 \\ \frac{E_A}{R} & 0 & \frac{1}{R} \end{pmatrix} \quad (8.15)$$

At the order x^2 the eigenvalues are

$$\begin{aligned} M_Z^2 &= \frac{v^2}{4} G^2 \left(1 - \frac{1 + \tilde{c}_{2\theta}^2}{\tilde{c}_\theta^2 - r} x^2 + \dots \right) \\ M_{L_3}^2 &= \frac{v^2}{4} \frac{G^2}{R} \left(1 + \frac{1 - 2r\tilde{s}_\theta^2 + \sqrt{\tilde{c}_{2\theta}^2 + 4r^2\tilde{s}_\theta^4}}{\tilde{c}_\theta^2 - r} x^2 + \dots \right) \\ M_{R_3}^2 &= \frac{v^2}{4} \frac{G^2}{R} \left(1 + \frac{1 - 2r\tilde{s}_\theta^2 - \sqrt{\tilde{c}_{2\theta}^2 + 4r^2\tilde{s}_\theta^4}}{\tilde{c}_\theta^2 - r} x^2 + \dots \right) \end{aligned} \quad (8.16)$$

The relation between the *hat* fields and the mass eigenstates is given by

$$\begin{pmatrix} \hat{W}_3 \\ \hat{V}_3 \\ \hat{A}_3 \end{pmatrix} = V \begin{pmatrix} Z \\ L_3 \\ R_3 \end{pmatrix} \quad (8.17)$$

with

$$V = \begin{pmatrix} N_1 & N_2 \frac{1 - \lambda_2 R_V}{E_V} & -N_3 \frac{1 - \lambda_3 R}{E_A} \\ N_1 \frac{E_V}{1 - R_V \lambda_1} & N_2 & -N_3 \frac{E_V}{E_A} \frac{1 - \lambda_3 R}{1 - \lambda_3 R_V} \\ -N_1 \frac{E_A}{1 - R \lambda_1} & -N_2 \frac{E_A}{E_V} \frac{1 - \lambda_2 R_V}{1 - \lambda_2 R} & N_3 \end{pmatrix} \quad (8.18)$$

where

$$\lambda_1 = 4 \frac{M_Z^2}{v^2 G^2}, \quad \lambda_2 = 4 \frac{M_{L_3}^2}{v^2 G^2}, \quad \lambda_3 = 4 \frac{M_{R_3}^2}{v^2 G^2} \quad (8.19)$$

and

$$\begin{aligned} N_1 &= \left(1 + \frac{E_V^2}{(1 - R_V \lambda_1)^2} + \frac{E_A^2}{(1 - R \lambda_1)^2} \right)^{-1/2} \\ N_2 &= \left(1 + \frac{(1 - R_V \lambda_2)^2}{E_V^2} \left(1 + \frac{E_A^2}{(1 - R \lambda_2)^2} \right) \right)^{-1/2} \\ N_3 &= \left(1 + \frac{(1 - R \lambda_3)^2}{E_A^2} \left(1 + \frac{E_V^2}{(1 - R_V \lambda_3)^2} \right) \right)^{-1/2} \end{aligned} \quad (8.20)$$

Let us call \mathbf{N} the matrix which transforms the fields appearing in the lagrangian (8.1) into the neutral eigenstates

$$\begin{pmatrix} \gamma \\ Z \\ L_3 \\ R_3 \end{pmatrix} = \mathbf{N}^{-1} \begin{pmatrix} \tilde{Y} \\ \tilde{W}_3 \\ \tilde{L}_3 \\ \tilde{R}_3 \end{pmatrix} \quad (8.21)$$

In the limit of $r \rightarrow 0$ and small x , by retaining only the first order in x , we get

$$\begin{pmatrix} \gamma \\ Z \\ L_3 \\ R_3 \end{pmatrix} \simeq \begin{pmatrix} \tilde{c}_\theta & \tilde{s}_\theta & \sqrt{2}\tilde{s}_\theta x & \sqrt{2}\tilde{s}_\theta x \\ -\tilde{s}_\theta & \tilde{c}_\theta & \sqrt{2}\tilde{c}_\theta x & -\sqrt{2}\frac{\tilde{s}_\theta^2}{\tilde{c}_\theta} x \\ 0 & -\sqrt{2}x & 1 & 0 \\ -\sqrt{2}x\frac{\tilde{s}_\theta}{\tilde{c}_\theta} & 0 & 0 & 1 \end{pmatrix} \begin{pmatrix} \tilde{Y} \\ \tilde{W}_3 \\ \tilde{L}_3 \\ \tilde{R}_3 \end{pmatrix} \quad (8.22)$$

where we have used the eqs. (8.9), (8.11), (8.14) and (8.18). We see that Z , L_3 and R_3 are essentially aligned along the combinations $(\tilde{c}_\theta \tilde{W}_3 - \tilde{s}_\theta \tilde{Y})$, \tilde{L}_3 and \tilde{R}_3 respectively. Unlike the charged case, however, the physical state R_3 is not completely decoupled, in fact at the leading order, it possesses a tiny component along the \tilde{Y} direction. The L_3 state has in turn a small contribution from the \tilde{W}_3 field.

9 Fermionic couplings

From the charged part of the fermionic lagrangian given in eq. (3.6), by using the relations (8.6), we can read directly the couplings to the fermions

$$\mathcal{L}_{charged} = - \left(a_W W_\mu^- + a_L L_\mu^- \right) J_L^{(+)\mu} + \text{h.c.} \quad (9.1)$$

where

$$\begin{aligned} a_W &= \frac{\tilde{g}}{\sqrt{2}} C_{11} \\ a_L &= \frac{\tilde{g}}{\sqrt{2}} C_{12} \end{aligned} \quad (9.2)$$

where C_{ij} are the matrix elements of the matrix \mathbf{C} defined in eq. (8.6), and

$$J_L^{(\pm)\mu} = \bar{\psi}_L \gamma^\mu \tau^{(\pm)} \psi_L \quad (9.3)$$

with

$$\tau^{(\pm)} = \frac{\tau_1 \pm i\tau_2}{2} \quad (9.4)$$

Let us notice that the R^\pm are not coupled to the fermions. In fact one can easily check that they have no mixing whatsoever and therefore these states will be absolutely stable as ensured by the phase invariance $R^\pm \rightarrow \exp(\pm i\alpha)R^\pm$.

For the neutral part we get

$$\begin{aligned} \mathcal{L}_{neutral} &= - \left\{ \left[A J_L^{(3)\mu} + B J_{em}^\mu \right] Z_\mu + \left[C J_L^{(3)\mu} + D J_{em}^\mu \right] L_{3\mu} + \left[E J_L^{(3)\mu} + F J_{em}^\mu \right] R_{3\mu} \right. \\ &\quad \left. + e J_{em}^\mu \gamma_\mu \right\} \end{aligned} \quad (9.5)$$

where

$$e = \tilde{g}\tilde{s}_\theta \cos \psi \quad (9.6)$$

and

$$\begin{aligned}
A &= GV_{11} & B &= -G\tilde{s}_\theta^2(V_{11} + \frac{\tilde{c}_\theta}{\tilde{s}_\theta} \sin \psi V_{21}) \\
C &= GV_{12} & D &= -G\tilde{s}_\theta^2(V_{12} + \frac{\tilde{c}_\theta}{\tilde{s}_\theta} \sin \psi V_{22}) \\
E &= GV_{13} & F &= -G\tilde{s}_\theta^2(V_{13} + \frac{\tilde{c}_\theta}{\tilde{s}_\theta} \sin \psi V_{23})
\end{aligned} \tag{9.7}$$

with V_{ij} are the matrix element of the matrix V given in eq. (8.18). In the usual limit we get, at the order x^2 ,

$$\begin{aligned}
A &\simeq G(1 - \frac{\tilde{s}_\theta^4 + \tilde{c}_\theta^4}{\tilde{c}_\theta^2} x^2) & B &\simeq -G\tilde{s}_\theta^2(1 - \frac{1 - 2\tilde{c}_\theta^4}{\tilde{c}_\theta^2} x^2) \\
C &\simeq -\sqrt{2}G\tilde{c}_\theta x & D &\simeq 0 \\
E &\simeq \sqrt{2}G\frac{\tilde{s}_\theta^2}{\tilde{c}_\theta} x & F &\simeq -\sqrt{2}G\frac{\tilde{s}_\theta^2}{\tilde{c}_\theta} x
\end{aligned} \tag{9.8}$$

10 Trilinear couplings

Starting from the original trilinear couplings given in eq. (3.4) and using the relations (8.6) and (8.21), we can evaluate all the trilinear couplings among the physical particles of the model. We get

$$\begin{aligned}
\mathcal{L}^{kin(3)} &= i \sum_{a,i,j} g_{O_a V_i^+ V_j^-} [O_a^{\mu\nu} V_{i\mu}^- V_{j\nu}^+ + O_a^\nu (V_{i\mu\nu}^- V_{j\mu}^+ - V_{i\mu\nu}^+ V_{j\mu}^-)] \\
&\quad + i \sum_a g_{O_a R^+ R^-} [O_a^{\mu\nu} R_\mu^- R_\nu^+ + O_a^\nu (R_{\mu\nu}^- R_\mu^+ - R_{\mu\nu}^+ R_\mu^-)]
\end{aligned} \tag{10.1}$$

where $O_a = \gamma, Z, L_3, R_3$ ($a = 1, 2, 3, 4$), $V_i^\pm = W^\pm, L^\pm$ ($i = 1, 2$) and

$$g_{O_a V_i^+ V_j^-} = g''(x C_{1i} C_{1j} N_{2a} + \frac{1}{\sqrt{2}} C_{2i} C_{2j} N_{3a}) \tag{10.2}$$

$$g_{O_a R^+ R^-} = g'' \frac{1}{\sqrt{2}} N_{4a} \tag{10.3}$$

As we noticed in the previous section, there are no mixings of the \tilde{R}^\pm with \tilde{W}^\pm and \tilde{L}^\pm (see eq. (8.1)), as a consequence there are no trilinear couplings involving a single charged R particle. Furthermore it is easy to check that $g_{\gamma W^+ L^-} = 0$.

11 Renormalization procedure

To identify the physical quantities in our model we proceed in the same way as in sect. 5. We again choose as input parameters the following physical constants: the electric charge, the mass of the Z and the Fermi constant.

Concerning the Fermi constant there is a general proof in ref. [4] stating that its relation with v^2 is the same of the SM one. Let us summarize the principal steps of the proof. Keeping into account the W^\pm and L^\pm exchanges in the μ -decay process, the Fermi constant is given by

$$\frac{G_F}{\sqrt{2}} = \frac{\tilde{g}^2}{8} \left(\frac{C_{11}^2}{M_{W^\pm}^2} + \frac{C_{12}^2}{M_{L^\pm}^2} \right) = \frac{\tilde{g}^2}{8} (M_{charged}^2)_{11}^{-1} = \frac{1}{2v^2} \quad (11.1)$$

where C_{ij} are given in eq. (8.6) and $M_{charged}^2$ in (8.3). The second equality in the previous equation follows from the relation

$$\mathbf{C}(M_D^2)^{-1}\mathbf{C}^{-1} = (M_{charged}^2)^{-1} \quad (11.2)$$

where M_D^2 is the diagonal form of the charged mass matrix. Recalling that the electric charge and the mass of the Z are given by

$$e = \tilde{g}\tilde{s}_\theta \cos \psi \quad (11.3)$$

$$M_Z^2 = \tilde{M}_Z^2 \lambda_1 \quad (11.4)$$

with

$$\tilde{M}_Z^2 = \frac{1}{4} v^2 \frac{\tilde{g}^2}{\tilde{c}_\theta^2} \quad (11.5)$$

and λ_1 is obtained by the diagonalization of the matrix in eq. (8.15).

By using the previous equations we can write the following relation ($\alpha = e^2/4\pi$)

$$\tilde{c}_\theta^2 \tilde{s}_\theta^2 = \frac{\pi\alpha}{\sqrt{2}G_F} \frac{1}{M_Z^2} \frac{\lambda_1}{\cos^2 \psi} \quad (11.6)$$

from which

$$\tilde{c}_\theta^2 = \frac{1}{2} + \sqrt{\frac{1}{4} - \frac{\pi\alpha}{\sqrt{2}G_F} \frac{1}{M_Z^2} \frac{\lambda_1}{\cos^2 \psi}} \quad (11.7)$$

From eq. (8.12) and using eq. (11.3) we obtain

$$\sin \psi = 2 \frac{e}{g''} \quad (11.8)$$

from which

$$\tilde{g} = \frac{e}{\tilde{s}_\theta \sqrt{1 - \frac{4e^2}{g''^2}}} \quad (11.9)$$

Let us notice that eq. (11.7), after using (11.9), involves only the angle $\tilde{\theta}$ and the measured quantities. Solving this equation in $\tilde{\theta}$ we can obtain \tilde{g} with the help of eq. (11.9). In this way all the original parameters of the lagrangian are expressed in terms of the observed quantities. In the numerical work we solve the equation (11.7) by iteration taking advantage of the fact that in the limit $g'' \rightarrow \infty$ we get back the SM. One can also solve the equation perturbatively in x . It is easy to verify that, at the order x^2 and at the first order in r (see eq. (8.4)), the procedure coincides with the one of sect. 5, and one recovers the equation (5.15). In fact this follows immediately from the expansion of λ_1 (see eqs. (8.19) and (8.16)) and $\cos^2 \psi$ at the same order

$$\lambda_1 \simeq 1 - z_z \left(1 + \frac{M_Z^2}{M^2}\right) \quad \cos^2 \psi \simeq 1 - z_\gamma \quad (11.10)$$

12 Widths

In the neutral sector the couplings of the fermions to the gauge bosons are

$$-\frac{1}{2}\bar{\psi}[(v_Z^f + \gamma_5 a_Z^f)\gamma_\mu Z^\mu + (v_{L_3}^f + \gamma_5 a_{L_3}^f)\gamma_\mu L_3^\mu + (v_{R_3}^f + \gamma_5 a_{R_3}^f)\gamma_\mu R_3^\mu]\psi \quad (12.1)$$

where v^f and a^f are the vector and axial vector couplings given by

$$\begin{aligned} v_Z^f &= AT_3^L + 2BQ_{em} \\ a_Z^f &= AT_3^L \\ v_{L_3}^f &= CT_3^L + 2DQ_{em} \\ a_{L_3}^f &= CT_3^L \\ v_{R_3}^f &= ET_3^L + 2FQ_{em} \\ a_{R_3}^f &= ET_3^L \end{aligned} \quad (12.2)$$

with A, B, C, D, E, F given in eq. (9.7). The total width of a vector boson V corresponding to the decay into fermion-antifermion is

$$\Gamma_V^{fermion} = \Gamma_V^h + 3(\Gamma_V^l + \Gamma_V^\nu) \quad (12.3)$$

where Γ_V^h includes the contribution of all the allowed quark-antiquark decays. The partial widths are given by

$$\Gamma_V^f = \frac{M_V}{48\pi} F(m_f^2/M_V^2) \quad (12.4)$$

with

$$F(r_f) = (1 - 4r_f)^{1/2}((v_V^f)^2(1 + 2r_f) + (a_V^f)^2(1 - 4r_f)) \quad (12.5)$$

and m_f the mass of the fermion.

The other possible decay channel for a neutral vector boson V is the one corresponding to the decay into a WW pair. The partial width is

$$\begin{aligned} \Gamma_V^W &= \frac{M_V}{192\pi} g_{VW+W}^2 \left(1 - 4\frac{M_W^2}{M_V^2}\right)^{3/2} \left(\frac{M_V}{M_W}\right)^4 \\ &\times \left[1 + 20\left(\frac{M_W}{M_V}\right)^2 + 12\left(\frac{M_W}{M_V}\right)^4\right] \end{aligned} \quad (12.6)$$

Concerning the charged resonances, only the L^\pm decay into fermions (see sect. 9). The leptonic width neglecting the fermionic mass corrections, is

$$\Gamma(L^- \rightarrow l\bar{\nu}_l) = \frac{1}{24\pi} a_L^2 M_L \equiv \Gamma_L^0 \quad (12.7)$$

with a_L given in eq. (9.2).

The decays into quark pairs are given by

$$\Gamma(L^- \rightarrow q'\bar{q}) = 3|V_{qq'}|^2 \Gamma_L^0 \quad (12.8)$$

where $V_{qq'}$ are the relevant Kobayashi-Maskawa matrix elements. In the case of the $b\bar{t}$ decay, we have taken into account the correction from the mass of the top

$$\Gamma(L^- \rightarrow b\bar{t}) = 3|V_{tb}|^2 \left(1 - \frac{3}{2}r_t + \frac{1}{2}r_t^3\right) \Gamma_L^0 \quad (12.9)$$

where $r_t = m_t^2/M_L^2$.

The other possible decay channel for L^\pm is the one corresponding to the decay into a WZ pair. The partial width is

$$\begin{aligned} \Gamma_L^{WZ} &= \frac{M_L}{192\pi} g_{ZW+L^-}^2 \left[\left(1 - \frac{M_Z^2 - M_W^2}{M_L^2}\right)^2 - 4\frac{M_W^2}{M_L^2} \right]^{3/2} \left(\frac{M_L^4}{M_W^2 M_Z^2} \right) \\ &\times \left[1 + 10 \left(\frac{M_W^2 + M_Z^2}{M_L^2} \right) + \frac{M_W^4 + M_Z^4 + 10M_W^2 M_Z^2}{M_L^4} \right] \end{aligned} \quad (12.10)$$

Let us now give the previous formulae for the widths in the $g'' \rightarrow \infty$ limit (at the order $(g/g'')^2$) and neglecting the mass corrections. For the fermionic channel we get

$$\begin{aligned} \Gamma(L_3 \rightarrow e^+ e^-) &= \frac{\sqrt{2}G_F M_W^2}{12\pi} M_{L_3} \left(\frac{g}{g''} \right)^2 \\ \Gamma(R_3 \rightarrow e^+ e^-) &= \frac{5\sqrt{2}G_F M_W^2}{12\pi} \frac{s_\theta^4}{c_\theta^4} M_{R_3} \left(\frac{g}{g''} \right)^2 \\ \Gamma(L^\pm \rightarrow e\bar{\nu}) &= \frac{\sqrt{2}G_F M_W^2}{6\pi} M_{L^\pm} \left(\frac{g}{g''} \right)^2 \end{aligned} \quad (12.11)$$

and the total fermionic widths are

$$\begin{aligned} \Gamma_{L_3}^{fermion} &= \frac{2\sqrt{2}G_F M_W^2}{\pi} M_{L_3} \left(\frac{g}{g''} \right)^2 \\ \Gamma_{R_3}^{fermion} &= \frac{10\sqrt{2}G_F M_W^2}{3\pi} \frac{s_\theta^4}{c_\theta^4} M_{R_3} \left(\frac{g}{g''} \right)^2 \\ \Gamma_{L^\pm}^{fermion} &= \frac{2\sqrt{2}G_F M_W^2}{\pi} M_{L^\pm} \left(\frac{g}{g''} \right)^2 \end{aligned} \quad (12.12)$$

By reading the relevant trilinear gauge couplings from eq. (10.2), and performing the same limit we have (with r defined in (8.4))

$$\begin{aligned} g_{L_3 W^+ W^-} &\simeq \sqrt{2}\tilde{g} r \frac{g}{g''} \\ g_{R_3 W^+ W^-} &\simeq \sqrt{2}\frac{\tilde{s}_\theta^2}{\tilde{c}_\theta^2}\tilde{g} r \frac{g}{g''} \\ g_{ZW+L^-} &\simeq \sqrt{2}\frac{\tilde{g}}{\tilde{c}_\theta} r \frac{g}{g''} \end{aligned} \quad (12.13)$$

Then, substituting in eqs. (12.6) and (12.10), we get

$$\begin{aligned} \Gamma_{L_3}^{WW} &= \frac{\sqrt{2}G_F M_W^2}{24\pi} M_{L_3} \left(\frac{g}{g''} \right)^2 \\ \Gamma_{R_3}^{WW} &= \frac{\sqrt{2}G_F M_W^2}{24\pi} \frac{s_\theta^4}{c_\theta^4} M_{R_3} \left(\frac{g}{g''} \right)^2 \\ \Gamma_{L^\pm}^{WZ} &= \frac{\sqrt{2}G_F M_W^2}{24\pi} M_{L^\pm} \left(\frac{g}{g''} \right)^2 \end{aligned} \quad (12.14)$$

It may be useful to compare the widths of \mathbf{L}_μ and \mathbf{R}_μ into vector boson pairs with those into fermions:

$$\begin{aligned}\Gamma_{L_3}^{fermion} &= 48 \Gamma_{L_3}^{WW} \\ \Gamma_{R_3}^{fermion} &= 80 \Gamma_{R_3}^{WW} \\ \Gamma_{L^\pm}^{fermion} &= 48 \Gamma_{L^\pm}^{WZ}\end{aligned}\tag{12.15}$$

We see that the total fermionic channel is dominant due to the multiplicity.

We conclude this section with some remarks about the decay of the vector mesons \mathbf{L}_μ and \mathbf{R}_μ . In the present, effective, description of the electroweak symmetry-breaking, the Goldstone bosons described by the field U given in eq. (2.12) become unphysical scalars eaten up by the ordinary gauge vector bosons W and Z . The absence of couplings among U and the states L and R results in a suppression of the decay rate of these states into W and Z . Consider, for instance, the decay of the new neutral gauge bosons into a W pair. In a model with only vector resonances this decay channel is largely the dominant one. The corresponding width is indeed given by [15]

$$\Gamma(V_0 \rightarrow WW) = \frac{\sqrt{2}G_F M^5}{192\pi M_W^2} \left(\frac{g}{g''}\right)^2\tag{12.16}$$

and it is enhanced with respect to the partial width into a fermion pair, by a factor $(M/M_W)^4$ [15]

$$\Gamma(V_0 \rightarrow \bar{f}f) \approx G_F M_W^2 \left(\frac{g}{g''}\right)^2 M\tag{12.17}$$

This fact is closely related to the existence of a coupling of order g'' among V_0 and the unphysical scalars absorbed by the W boson. Indeed the fictitious width of V_0 into these scalars provides, via the equivalence theorem [16], a good approximation to the width of V_0 into a pair of longitudinal W and it is precisely given by eq. (12.16).

On the contrary, if there is no direct coupling among the new gauge bosons and the would-be Goldstone bosons which provide the longitudinal degree of freedom to the W , then their partial width into longitudinal W 's will be suppressed compared to the leading behaviour in eq. (12.16), and the width into a W pair could be similar to the fermionic width. In fact, as we have explicitly checked (see eq. (12.13)) the trilinear couplings between the new gauge bosons and a W pair is no longer of order (g/g'') , but of the order $(g/g'') r$. The same argument also holds for the charged case.

Numerically, the comparison between the degenerate case (D-model) and the BESS model with only vector resonances (V-model) is shown in Table I, for a choice of the parameters of the model ($M_{L^+} = 1 \text{ TeV}$, $g'' = 13$ and no direct coupling of L^+ to fermions). The V-model features an enhancement of the WZ channel, common to the usual strong interacting models. The D-model has no such an enhancement.

As already noticed, in usual strong interacting models an enhancement of $W_L W_L$ scattering is expected. Due to the previous considerations, our case is quite different. If we study $W_L W_L$ scattering the lowest order result violates unitarity at energies above 1.7 TeV , as in the standard model in the formal limit $m_H \rightarrow \infty$. So we expect our model to be valid only up to energies of this order.

D-model	Γ_{L^+} (GeV)	$\text{Br}(L^+ \rightarrow e\nu)$	$\text{Br}(L^+ \rightarrow ud)$	$\text{Br}(L^+ \rightarrow WZ)$
	0.18	8.1×10^{-2}	2.4×10^{-1}	2.2×10^{-2}
V-model	Γ_{V^+} (GeV)	$\text{Br}(V^+ \rightarrow e\nu)$	$\text{Br}(V^+ \rightarrow ud)$	$\text{Br}(V^+ \rightarrow WZ)$
	12.1	5.9×10^{-4}	1.7×10^{-3}	9.9×10^{-1}

Table I: Comparison between the degenerate BESS model (D-model) and the BESS model with only vector resonances (V-model) for the total width and branching ratios of L^+ (D-model) and V^+ (V-model) with the choice of parameters: $M = 1$ TeV, $g'' = 13$ and no direct coupling of L^+/V^+ to fermions.

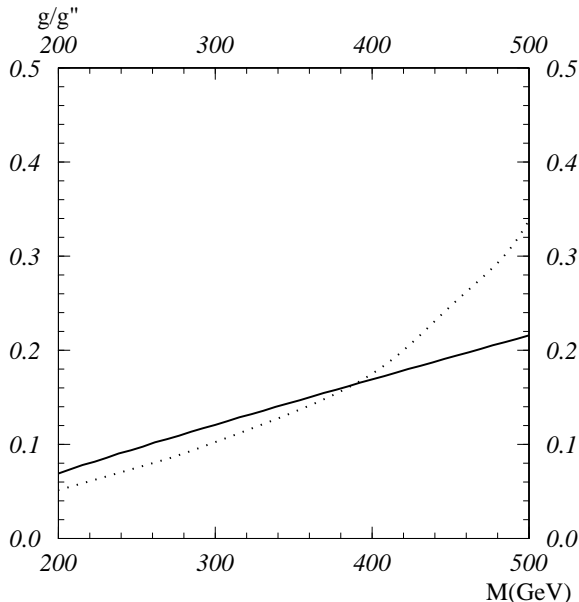


Fig. 3 - 95% C.L. upper bounds on g/g'' vs. M from LEP data (continuous line) and CDF (dotted line). LEP bounds are obtained from the ϵ parameters, while CDF limits come from $\sigma B(p\bar{p} \rightarrow \ell\nu)$ at $\sqrt{s} = 1.8$ TeV and with an integrated luminosity of 19.7pb^{-1} .

13 Degenerate BESS at Tevatron

Data from the Fermilab Tevatron Collider, collected by the CDF collaboration [17] establish limits on the model parameter space. Their search was done through the decay $W' \rightarrow e\nu$, assuming standard couplings of the W' to the fermions. Their result can be easily translated into a limit for the degenerate BESS model parameter space.

In Fig. 3 these limits are shown in terms of the mass of the R^\pm resonance (equivalent to M , see eq. (8.2)) and the ratio of coupling constants g/g'' . Actually the parameter of the model is x as given in eq. (8.4). Here, for simplicity of notation, we call it g/g'' . The limit from CDF (dotted line) is compared with the result obtained from LEP (continuous line). The excluded region is above the two curves. The figure was obtained using the CDF 95% C.L. limit on the W' cross-section times the branching ratio and comparing this limit with the predictions of our model at fixed g/g'' , thus giving a limit for the R^\pm mass. This procedure was then iterated for various values of g/g'' . The statistical significance of the plot is that of a 95% C.L. limit in one variable, the mass, at a given value of g/g'' .

The limit from CDF is more restrictive for low resonance masses, while LEP limit is more restrictive for higher mass values.

14 Degenerate BESS at e^+e^- colliders

We have considered the sensitivity of the model at LEP2 and future e^+e^- linear colliders, for different options of total centre of mass energies and luminosities.

We have analyzed cross-sections and asymmetries for the channel $e^+e^- \rightarrow f^+f^-$ and $e^+e^- \rightarrow W^+W^-$ in the Standard Model and in the degenerate BESS model at tree level. The BESS states relevant for the analysis at e^+e^- colliders are L_3 and R_3 . The two vector bosons are degenerate in mass in the large g'' limit. The L_3 mass is larger than the R_3 mass due to terms of the order $(g/g'')^2$ and higher (see eq. (8.16)).

If the masses of the resonances are below and not very far from the collider energy, due to beamstrahlung and synchrotron radiation, in a high energy collider, one expects to see two very close narrow peaks below the maximum c.m. energy even without having to tune the beam energies. However in this paper we do not consider the direct production of R_3 and L_3 from e^+e^- . If instead the masses are higher than the maximum c.m. energy, they will give rise to indirect effects in the $e^+e^- \rightarrow f^+f^-$ and $e^+e^- \rightarrow W^+W^-$ cross-sections, which we discuss below.

For the purposes of our calculation we have assumed that it will be possible to separate $e^+e^- \rightarrow W_L^+W_L^-$, $e^+e^- \rightarrow W_L^+W_T^-$, and $e^+e^- \rightarrow W_T^+W_T^-$. A similar analysis for the BESS model with only vector resonances was given in ref. [15].

In the fermion channel our study is based on the following observables:

$$\begin{aligned} & \sigma^\mu, \quad \sigma^h \\ & A_{FB}^{e^+e^- \rightarrow \mu^+\mu^-}, \quad A_{FB}^{e^+e^- \rightarrow \bar{b}b} \\ & A_{LR}^{e^+e^- \rightarrow \mu^+\mu^-}, \quad A_{LR}^{e^+e^- \rightarrow \bar{b}b}, \quad A_{LR}^{e^+e^- \rightarrow had} \end{aligned} \tag{14.1}$$

where A_{FB} and A_{LR} are the forward-backward and left-right asymmetries, and $\sigma^{h(\mu)}$ is the total hadronic ($\mu^+\mu^-$) cross-section.

The total cross-section for the process $e^+e^- \rightarrow f^+f^-$ is given by (at tree level)

$$\sigma = \frac{s}{3 \cdot 256\pi} \sum_{h_f, h_e} |F(h_f, h_e)|^2 \tag{14.2}$$

with

$$F(h_f, h_e) = -\frac{4eq_f}{s} + \sum_{a=Z, L_3, R_3} \frac{(v_a^f + h_f a_a^f)(v_a + h_e a_a)}{s - M_a^2 + iM_a \Gamma_a} \tag{14.3}$$

where $h_{f,e} = \pm 1$ are the helicities of f and e respectively, q_f is the electric charge of f , $v_a = v_a^e$, $a_a = a_a^e$, with $a = Z, L_3, R_3$, and Γ_a are the widths of the neutral gauge bosons. The partial widths of the L_3 and R_3 bosons corresponding to decays into fermion-antifermion and WW are given in sect. 12.

The forward-backward asymmetry in the present case is given by

$$A_{FB}^{e^+e^- \rightarrow f^+f^-} = \frac{3(1-P) \sum_{h_f, h_e} h_f h_e |F(h_f, h_e)|^2 + 2P \sum_{h_f} h_f |F(h_f, 1)|^2}{4(1-P) \sum_{h_f, h_e} |F(h_f, h_e)|^2 + 2P \sum_{h_f} |F(h_f, 1)|^2} \quad (14.4)$$

where P is the degree of longitudinal polarization of the electron beam.

The left-right asymmetry is given by

$$A_{LR}^{e^+e^- \rightarrow f^+f^-} = P \frac{\sum_{h_f, h_e} h_e |F(h_f, h_e)|^2}{\sum_{h_f, h_e} |F(h_f, h_e)|^2} \quad (14.5)$$

The notations are the same as for the forward-backward asymmetry.

In our study we consider also the WW channel, with one W decaying leptonically and the other hadronically. The reason for choosing this decay channel is to get a clean signal to reconstruct the polarization of the W 's (see for example [18]). For the $e^+e^- \rightarrow WW$ channel the relevant observables are:

$$A_{LR}^{e^+e^- \rightarrow W^+W^-} = \left(\frac{d\sigma}{d\cos\theta}(P_e = +P) - \frac{d\sigma}{d\cos\theta}(P_e = -P) \right) / \frac{d\sigma}{d\cos\theta} \quad (14.6)$$

where θ is the e^+e^- center of mass scattering angle. Assuming that the final W polarization can be reconstructed by using the W decay distributions, it is convenient to consider the cross-sections for $W_L W_L$, $W_T W_L$, $W_T W_T$ and the corresponding left-right asymmetries as additional observables [19].

In the e^+e^- center of mass frame the angular distribution $d\sigma/d\cos\theta$ and the left-right asymmetry read [20]

$$\begin{aligned} \frac{d\sigma}{d\cos\theta} &= \frac{p}{64\pi\sqrt{s}} \left\{ a_W^4 \left[\frac{4}{M_W^2} + p^2 \sin^2\theta \left(\frac{1}{M_W^4} + \frac{4}{t^2} \right) \right] \right. \\ &+ 2F_1 p^2 \left[\frac{4s}{M_W^2} + \left(3 + \frac{sp^2}{M_W^4} \right) \sin^2\theta \right] \\ &+ \left. F_1' \left[8 \left(1 + \frac{M_W^2}{t} \right) + 16 \frac{p^2}{M_W^2} + \frac{p^2}{s} \sin^2\theta \left(\frac{s^2}{M_W^4} - 2 \frac{s}{M_W^2} - 4 \frac{s}{t} \right) \right] \right\} \end{aligned} \quad (14.7)$$

$$(14.8)$$

and

$$\begin{aligned} A_{LR}(\cos\theta) &= -P \frac{p}{64\pi\sqrt{s}} \left\{ a_W^4 \left[\frac{4}{M_W^2} + p^2 \sin^2\theta \left(\frac{1}{M_W^4} + \frac{4}{t^2} \right) \right] \right. \\ &+ 2F_2 p^2 \left[\frac{4s}{M_W^2} + \left(3 + \frac{sp^2}{M_W^4} \right) \sin^2\theta \right] \\ &+ F_1' \left[8 \left(1 + \frac{M_W^2}{t} \right) + 16 \frac{p^2}{M_W^2} \right. \\ &+ \left. \left. \frac{p^2}{s} \sin^2\theta \left(\frac{s^2}{M_W^4} - 2 \frac{s}{M_W^2} - 4 \frac{s}{t} \right) \right] \right\} / \frac{d\sigma}{d\cos\theta} \end{aligned} \quad (14.9)$$

$$(14.10)$$

where

$$\begin{aligned}
p &= \frac{1}{2}\sqrt{s}(1 - 4M_W^2/s)^{1/2} \\
t &= M_W^2 - \frac{1}{2}s[1 - \cos\theta(1 - 4M_W^2/s)^{1/2}]
\end{aligned} \tag{14.11}$$

The quantity a_W is given in (9.2) and

$$\begin{aligned}
F_1 &= \left(\frac{2e^2}{s}\right)^2 + \sum_{a=Z,L_3,R_3} [(v_a^2 + a_a^2)g_{aWW}^2 \frac{1}{(s - M_a^2)^2 + M_a^2\Gamma_a^2} \\
&\quad - 4\frac{e^2}{s}v_a g_{aWW} \frac{s - M_a^2}{(s - M_a^2)^2 + M_a^2\Gamma_a^2}] \\
&\quad + \sum_{a,b=Z,L_3,R_3}^{a \neq b} (v_a v_b + a_a a_b) g_{aWW} g_{bWW} \\
&\quad \frac{(s - M_a^2)(s - M_b^2) + M_a \Gamma_a M_b \Gamma_b}{[(s - M_a^2)^2 + M_a^2\Gamma_a^2][(s - M_b^2)^2 + M_b^2\Gamma_b^2]}
\end{aligned} \tag{14.12}$$

$$F_1' = a_W^2 \left[\frac{-2e^2}{s} + \sum_{a=Z,L_3,R_3} g_{aWW} (v_a + a_a) \frac{s - M_a^2}{(s - M_a^2)^2 + M_a^2\Gamma_a^2} \right] \tag{14.13}$$

$$\begin{aligned}
F_2 &= -\frac{4e^2}{s} \sum_{a=Z,L_3,R_3} a_a g_{aWW} \frac{s - M_a^2}{(s - M_a^2)^2 + M_a^2\Gamma_a^2} \\
&\quad + 2 \sum_{a=Z,L_3,R_3} a_a v_a g_{aWW}^2 \frac{1}{(s - M_a^2)^2 + M_a^2\Gamma_a^2} \\
&\quad + \sum_{a,b=Z,L_3,R_3}^{a \neq b} (a_a v_b + v_a a_b) g_{aWW} g_{bWW} \\
&\quad \frac{(s - M_a^2)(s - M_b^2) + M_a \Gamma_a M_b \Gamma_b}{[(s - M_a^2)^2 + M_a^2\Gamma_a^2][(s - M_b^2)^2 + M_b^2\Gamma_b^2]}
\end{aligned} \tag{14.14}$$

where g_{ZWW} , g_{L_3WW} and g_{R_3WW} are given in eq. (10.2).

The cross-sections for $W_L W_L$, $W_T W_L$, and $W_T W_T$ are:

$$\begin{aligned}
\frac{d\sigma_{LL}}{d\cos\theta} &= \frac{p}{64\pi\sqrt{s}} \left\{ \frac{a_W^4}{16M_W^4} \frac{1}{t^2} [s^3(1 + \cos^2\theta) - 4M_W^4(3s + 4M_W^2)] \right. \\
&\quad - 4(s + 2M_W^2)p\sqrt{s}\cos\theta \sin^2\theta \\
&\quad + \frac{F_1}{8M_W^4} \sin^2\theta (s^3 - 12sM_W^4 - 16M_W^6) \\
&\quad + F_1' \sin^2\theta \frac{1}{2t} [ps\sqrt{s}\cos\theta \frac{1}{2M_W^4} (s + 2M_W^2) \\
&\quad \left. - \frac{1}{4M_W^4} (s^3 - 12sM_W^4 - 16M_W^6)] \right\}
\end{aligned} \tag{14.15}$$

$$\begin{aligned}
\frac{d\sigma_{TL}}{d\cos\theta} &= \frac{p}{64\pi\sqrt{s}} \left\{ a_W^4 \frac{1}{2t^2 M_W^2} [s^2(1 + \cos^4\theta) + 4M_W^4(1 + \cos^2\theta)] \right. \\
&\quad \left. - 4(4p^2 + s\cos^2\theta)p\sqrt{s}\cos\theta + 2s(s - 6M_W^2)\cos^2\theta - 4sM_W^2 \right\}
\end{aligned}$$

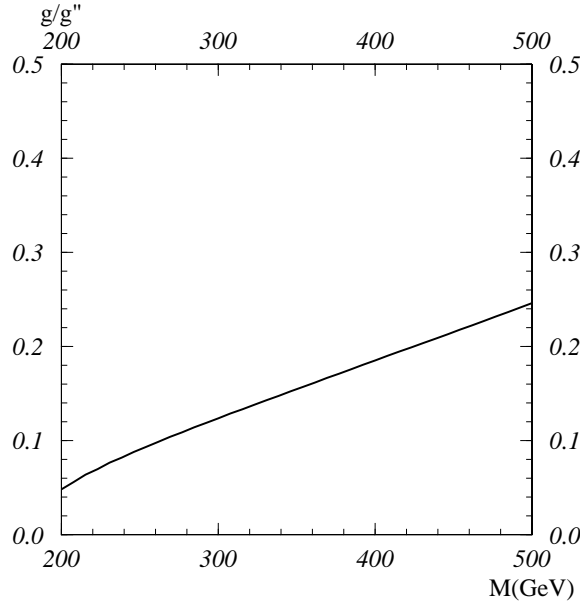


Fig. 4 - 90% C.L. contour on the plane $(M, g/g'')$ from LEP2. The limits are obtained considering $\sqrt{s} = 175$ GeV and with an integrated luminosity of 500pb^{-1} , combining the deviations of M_W , σ^μ , σ^h , A_{FB}^μ , A_{FB}^b .

$$\begin{aligned}
& + 4F_1 s \frac{p^2}{M_W^2} (1 + \cos^2 \theta) \\
& + 2F_1' \frac{p\sqrt{s}}{tM_W^2} [\cos \theta (4p^2 + s \cos^2 \theta) - 2p\sqrt{s} (1 + \cos^2 \theta)] \} \quad (14.16)
\end{aligned}$$

$$\begin{aligned}
\frac{d\sigma_{TT}}{d\cos\theta} & = \frac{p}{64\pi\sqrt{s}} \left\{ a_W^4 \frac{1}{t^2} [s(1 + \cos^2 \theta) - 2M_W^2 - 2p\sqrt{s} \cos \theta] \sin^2 \theta \right. \\
& \left. + 4F_1 p^2 \sin^2 \theta + F_1' \frac{\sin^2 \theta}{2t} [4p\sqrt{s} \cos \theta - 8p^2] \right\} \quad (14.17)
\end{aligned}$$

The left-right asymmetries for longitudinal and/or transverse polarized W can be easily obtained as in eq. (14.10) by substituting F_1 by F_2 in eqs. (14.15), (14.16), (14.17), and dividing by the corresponding differential cross-section. At LEP2 we can add to the previous observables the W mass measurement, coming from the $e^+e^- \rightarrow WW$ channel. In Fig. 4 we show a 90% C.L. contour plot in the parameter space of the model. The limits are obtained considering $\sqrt{s} = 175$ GeV and an integrated luminosity of 500pb^{-1} , combining the deviations of M_W , σ^μ , σ^h , A_{FB}^μ , A_{FB}^b . For M_W we assume a total error (statistical and systematic) $\Delta M_W = 50$ MeV. For σ^h the total error assumed is 2%. For the other observable quantities we assume only statistical errors. If the possibility of having polarized beams at LEP2 is considered, the improvement with respect to the unpolarized case is only marginal. Also, considering the option of LEP2 at $\sqrt{s} = 190$ GeV does not substantially alter the result. The comparison with LEP bounds (see Fig. 1) shows that LEP2 will not improve considerably the existing limits. Of course one has to be careful in this comparison, since in the case of LEP we have experimental values, whereas for LEP2 case the limits are obtained by using deviations from the SM results.

To further test the model is necessary to consider higher energy colliders. We study two options for a high energy e^+e^- collider: $\sqrt{s} = 500$ GeV with an integrated luminosity of 20fb^{-1} and $\sqrt{s} = 1$ TeV with an integrated luminosity of 80fb^{-1} .

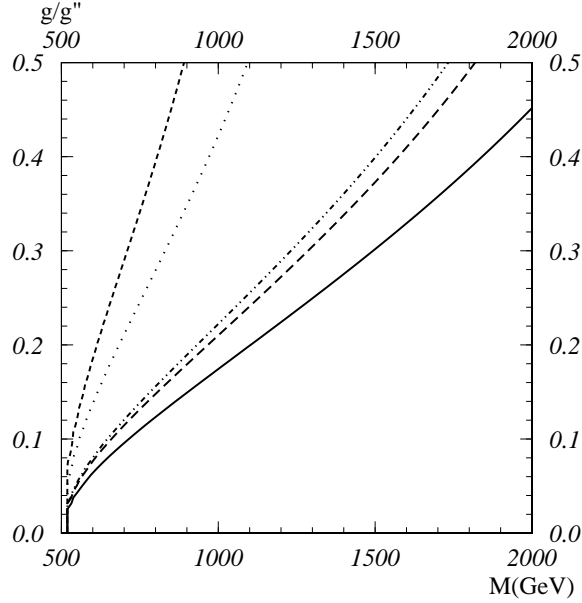


Fig. 5 - 90% C.L. contour on the plane $(M, g/g'')$ from e^+e^- at $\sqrt{s} = 500$ GeV with an integrated luminosity of 20fb^{-1} for various observables. The dashed-dotted line represents the limit from σ^h with an assumed error of 2%; the dashed line near to the preceding one is σ^μ (error 1.3%); the dotted line is A_{FB}^μ (error 0.5%); the uppermost dashed line is A_{FB}^b (error 0.9%). The continuous line represents the combined limits.

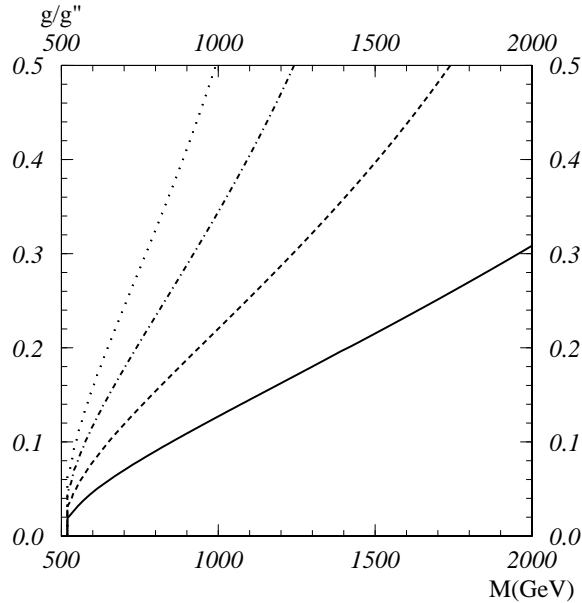


Fig. 6 - 90% C.L. contour on the plane $(M, g/g'')$ from e^+e^- at $\sqrt{s} = 500$ GeV with an integrated luminosity of 20fb^{-1} and a polarization of 0.5 for various observables. The dashed-dotted line represents the limit from A_{LR}^μ with an assumed error of 0.6%; the dashed line is A_{LR}^h (error 0.4%); the dotted line is A_{LR}^b (error 1.1%). The continuous is obtained by combining the polarized and the unpolarized observables: $\sigma^h, \sigma^\mu, A_{FB}^\mu, A_{FB}^b, A_{LR}^\mu, A_{LR}^h, A_{LR}^b$.

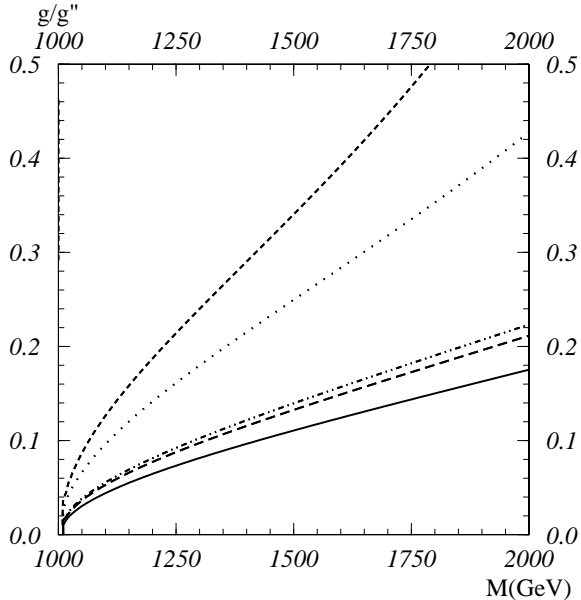


Fig. 7 - 90% C.L. contour on the plane $(M, g/g'')$ from e^+e^- at $\sqrt{s} = 1000$ GeV with an integrated luminosity of $80fb^{-1}$ for various observables. The dashed-dotted line represents the limit from σ^h with an assumed error of 2%; the dashed line near to the preceding one is σ^μ (error 1.3%); the dotted line is A_{FB}^μ (error 0.5%); the uppermost dashed line is A_{FB}^b (error 0.9%). The continuous line represents the combined limits.

In Fig. 5 we present the 90% C.L. contour on the plane $(M, g/g'')$ from e^+e^- at $\sqrt{s} = 500$ GeV with an integrated luminosity of $20fb^{-1}$ for various observables. The dashed-dotted line represents the limit from σ^h ; the dashed line near to the preceding one is σ^μ , the dotted line is A_{FB}^μ and the uppermost dashed line is A_{FB}^b . As it is evident more stringent bounds come from the cross-section measurements. Asymmetries give less restrictive bounds due to a compensation between the L_3 and R_3 exchange. By combining all the deviations in the previously considered observables we get the limit shown by the continuous line.

Polarized electron beams allow to get further limit in the parameter space as shown in Fig. 6. We neglect the error on the measurement of the polarization and use a polarization value equal to 0.5. The dashed-dotted line represents the limit from A_{LR}^μ , the dashed line from A_{LR}^h , the dotted line from A_{LR}^b . Combining all the polarized and unpolarized beam observables we get the bound shown by the continuous line. In conclusion we get a substantial improvement with respect to the LEP bounds, even without polarized beams.

The previous analysis has been repeated at $\sqrt{s} = 1$ TeV with an integrated luminosity of $80fb^{-1}$. The results are shown in Figs. 7 and 8.

In Fig. 9 we show a combined picture of the 90% C.L. contours on the plane $(M, g/g'')$ from e^+e^- at two values of \sqrt{s} . The dotted line represents the limit from the combined unpolarized observables at $\sqrt{s} = 500$ GeV with an integrated luminosity of $20fb^{-1}$; the dashed line is the limit from the combined unpolarized observables at $\sqrt{s} = 1000$ GeV with an integrated luminosity of $80fb^{-1}$. As expected increasing the energy of the collider and rescaling the integrated luminosity result in stronger bounds on the parameter space.

We have then studied the WW final state, considering the observables given in eq. (14.6). In Fig. 10 we show the plot from the combined WW observables. An angular cut has been imposed on W scattering angle ($|\cos\theta| \leq 0.95$) and 18 angular bins have

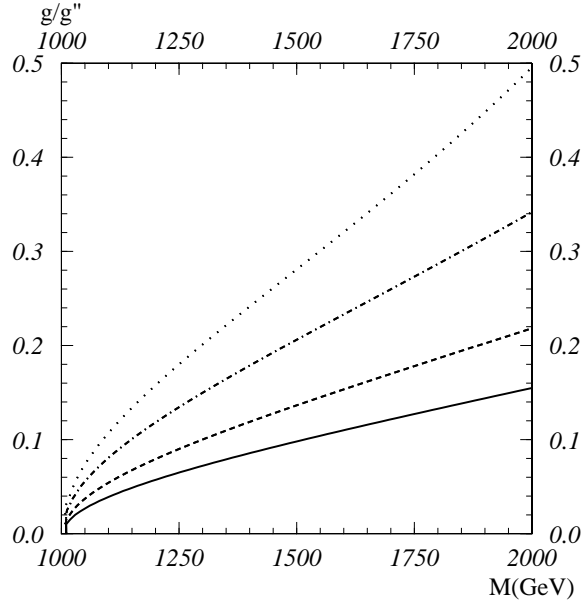


Fig. 8 - 90% C.L. contour on the plane $(M, g/g'')$ from e^+e^- at $\sqrt{s} = 1000$ GeV with an integrated luminosity of 80fb^{-1} and a polarization of 0.5 for various observables. The dashed-dotted line represents the limit from A_{LR}^μ with an assumed error of 0.6%; the dashed line is A_{LR}^h (error 0.4%); the dotted line is A_{LR}^b (error 1.1%). The continuous line is obtained by combining the polarized and the unpolarized observables: σ^h , σ^μ , A_{FB}^μ , A_{FB}^b , A_{LR}^μ , A_{LR}^h , A_{LR}^b .

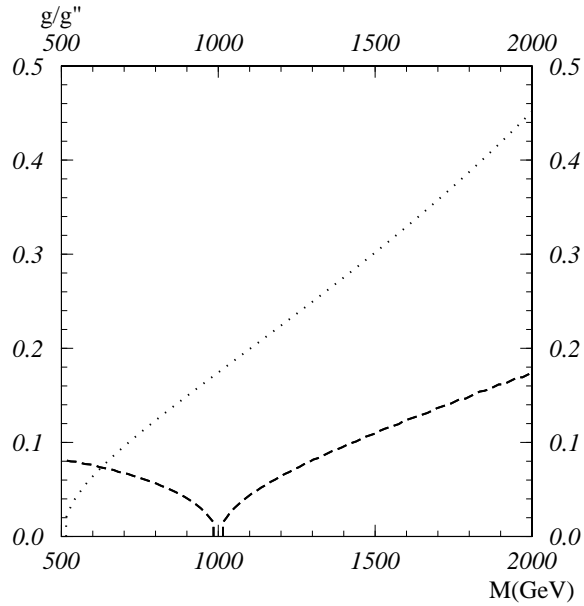


Fig. 9 - 90% C.L. contour on the plane $(M, g/g'')$ from e^+e^- at two \sqrt{s} values: the dotted line represents the limit from the combined unpolarized observables at $\sqrt{s} = 500$ GeV with an integrated luminosity of 20fb^{-1} ; the dashed line is the limit from the combined unpolarized observables at $\sqrt{s} = 1000$ GeV with an integrated luminosity of 80fb^{-1} .

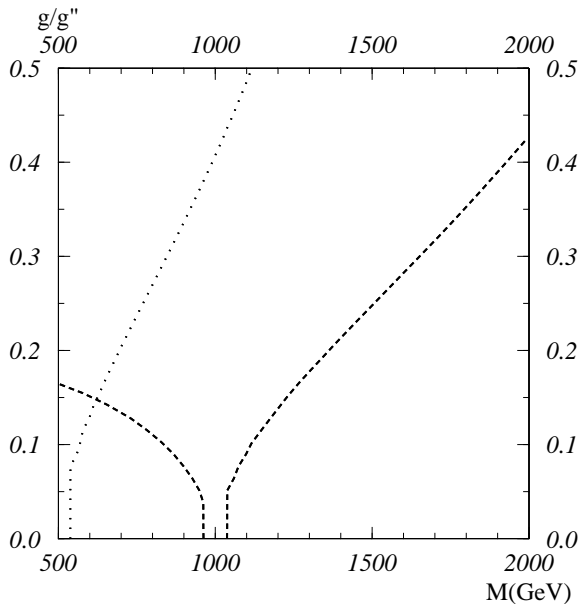


Fig. 10 - 90% C.L. contour on the plane $(M, g/g'')$ from WW differential cross-section and the corresponding left-right asymmetries, considering also the W polarization reconstruction. The dotted line represents the limit from $\sqrt{s} = 500$ GeV with an integrated luminosity of 20fb^{-1} ; the dashed line is the limit from $\sqrt{s} = 1000$ GeV with an integrated luminosity of 80fb^{-1} .

been considered. We have assumed an overall detection efficiency of 10% including the branching ratio $B = 0.29$ and a loss of luminosity from beamstrahlung. All these new bounds do not alter the strong limits obtained using the fermion final state. This is because, as we have already noticed, the degenerate model has no strong enhancement of the WW channel, present in the usual strong electroweak models.

15 Degenerate BESS at hadron colliders

The e^+e^- colliders give the possibility to explore the neutral sector of symmetry breaking by the production of the neutral vector and axial vector gauge bosons of the model. Hadron colliders are complementary to e^+e^- machines, in the sense that they also allow to study the new charged vector and axial vector resonances.

The physics of large hadron colliders has been extensively discussed in a number of papers (see for example [21] and references therein); such a machine will be able either to discover the new resonances or to constrain the physical region left unconstrained by previous data.

Let us consider first the case in which no new resonances are discovered. In this case limits can be imposed on the parameter space of the model. As a preliminary analysis we can consider the total cross-section of $pp \rightarrow L^\pm, W^\pm \rightarrow \ell\nu$ ($\ell = e, \mu$), which has a clear signature and a large number of events, to be compared with the standard model production of $\ell\nu$. We have calculated the total cross-section $pp \rightarrow L^\pm, W^\pm \rightarrow \ell\nu$ and, by comparing with the SM background, we have obtained a contour plot at 90% C.L. in the two variables M and g/g'' , shown in Fig. 11.

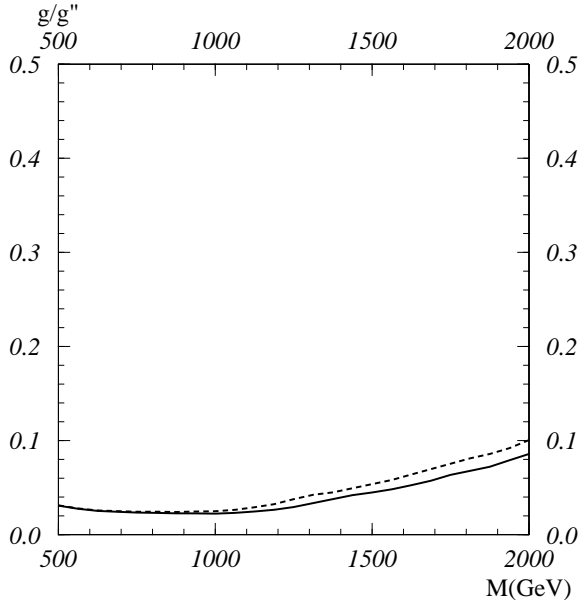


Fig. 11 - 90% C.L. contour on the plane $(M, g/g'')$ from total cross-section of $pp \rightarrow L^\pm, W^\pm \rightarrow \ell\nu$ ($\ell = e, \mu$). We have assumed a systematical error of 5% in the cross-section and the statistical error obtained considering a luminosity of $10^{34} \text{cm}^{-2} \text{s}^{-1}$ (continuous line) or a luminosity of $10^{33} \text{cm}^{-2} \text{s}^{-1}$ (dashed line) and one year run at LHC (10^7 s).

The applied cuts were $|p_{t\mu}| > \min(M_{L^\pm}/2 - 50 \text{ GeV}, 400 \text{ GeV})$ in order to maximize the deviation of BESS model cross-section with respect to the Standard Model one. In this analysis we do not optimize cuts and an improvement is still possible studying in more detail specific cases. We have assumed a systematical error of 5% in the cross-section and the statistical error obtained considering a luminosity of $10^{34} \text{cm}^{-2} \text{s}^{-1}$ (continuous line) or a luminosity of $10^{33} \text{cm}^{-2} \text{s}^{-1}$ (dashed line) and one year run (10^7 s) at LHC ($\sqrt{s} = 14 \text{ TeV}$). The new resonances of the model can be discovered directly for a wide range of values of the parameter space of the model. The discovery limit in the mass of the resonance depends on the value of g/g'' . For example if $g/g'' = 0.1$, the resonance is visible over the background at least up to 2 TeV , in the channel $pp \rightarrow \mu\nu$.

In Figs. 12-14 we show the differential distribution of events at LHC of $pp \rightarrow L^\pm, W^\pm \rightarrow \mu\nu$ in the transverse momentum of the muon for different values of M_{L^\pm} and g/g'' . As stated before we choose this channel due to the clean signature and the large cross-section. The events were simulated using Pythia Montecarlo [22]. A rough simulation of the detector was also performed. The energy of the leptons was smeared according to

$$\frac{\Delta E}{E} = 15\% \quad (15.1)$$

and the error in the 3-momentum determination was assumed of 5%.

In particular in Fig. 12 a spectacular case is presented for a low resonance mass $M_{L^\pm} = 500 \text{ GeV}$ and $g/g'' = 0.15$. The total L^\pm width is $\Gamma_{L^\pm} = 0.907 \text{ GeV}$, with the corresponding $B(L^+ \rightarrow \mu\nu) = 8.5 \times 10^{-2}$. The following cuts have been applied: $|p_{t\mu}|, |p_{t \text{ miss}}| > 150 \text{ GeV}$. The number of signal events per year is approximately 128000, the corresponding background consists of 51500 events.

In Fig. 13 we show a case corresponding to $M_{L^\pm} = 1 \text{ TeV}$, $g/g'' = 0.075$ and $\Gamma_{L^\pm} = 0.454 \text{ GeV}$. The following cuts have been applied: $|p_{t\mu}|, |p_{t \text{ miss}}| > 300 \text{ GeV}$ and $E_{\text{miss}} >$

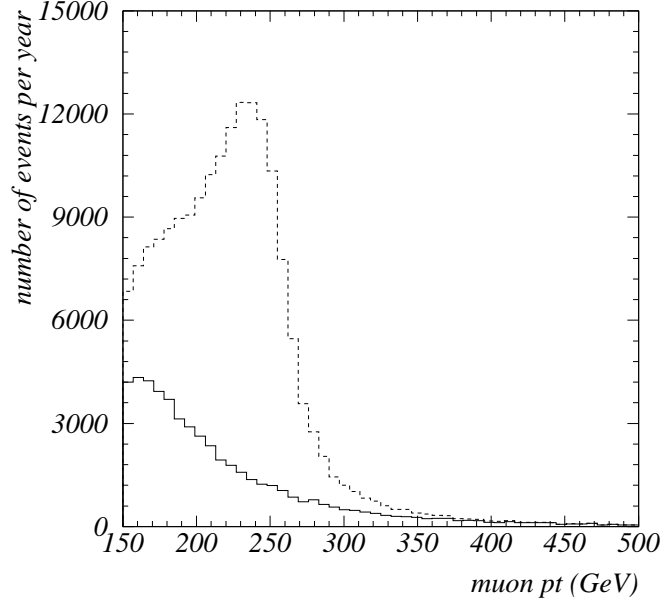


Fig. 12 - Differential distribution of $pp \rightarrow L^\pm, W^\pm \rightarrow \mu\nu$ events at LHC with a luminosity of $10^{34} \text{cm}^{-2} \text{s}^{-1}$, for $M_{L^\pm} = 500 \text{ GeV}$, $g/g'' = 0.15$. The following cuts have been applied: $|p_{t\mu}|, |p_{t \text{ miss}}| > 150 \text{ GeV}$. The continuous line represents the Standard Model background while the dashed one is the degenerate BESS model expectation.

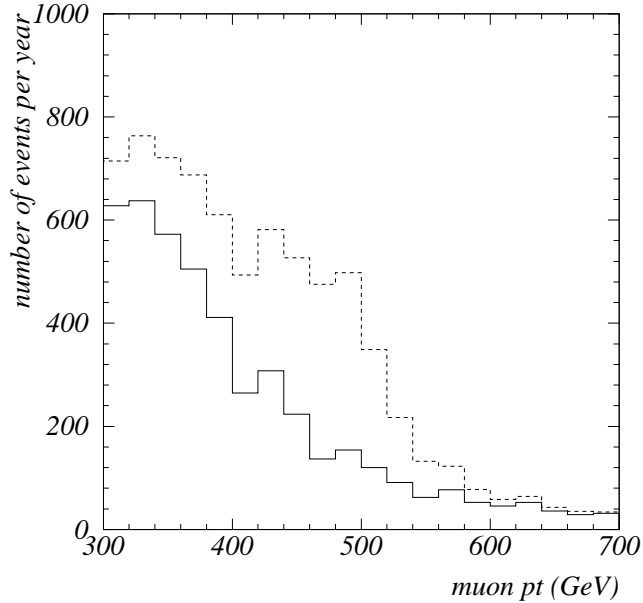


Fig. 13 - Differential distribution of $pp \rightarrow L^\pm, W^\pm \rightarrow \mu\nu$ events at LHC with a luminosity of $10^{34} \text{cm}^{-2} \text{s}^{-1}$, for $M_{L^\pm} = 1 \text{ TeV}$, $g/g'' = 0.075$. The following cuts have been applied: $|p_{t\mu}|, |p_{t \text{ miss}}| > 300 \text{ GeV}$. The continuous line is the Standard Model background, the dashed line represents the degenerate BESS model signal.

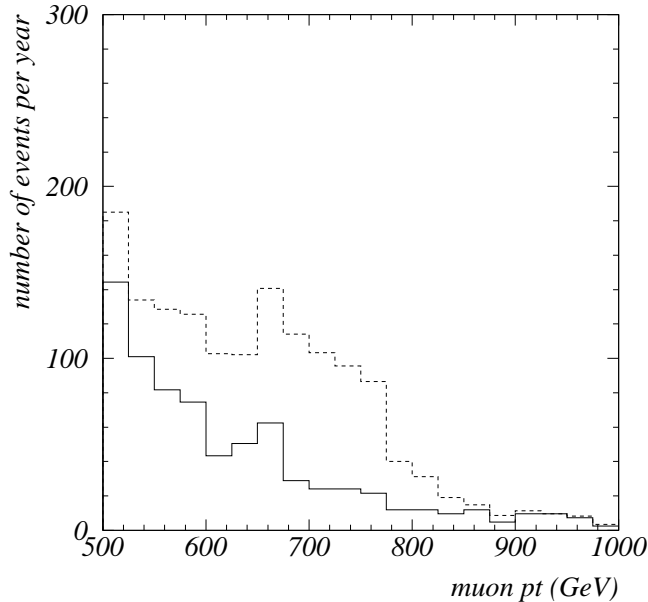


Fig. 14 - Differential distribution of $pp \rightarrow L^\pm, W^\pm \rightarrow \mu\nu$ events at LHC with a luminosity of $10^{34} \text{cm}^{-2} \text{s}^{-1}$, for $M_{L^\pm} = 1.5 \text{ TeV}$, $g/g'' = 0.1$. The following cuts have been applied: $|p_{t\mu}| > 400 \text{ GeV}$, $|p_{t \text{ miss}}| > 400 \text{ GeV}$. The continuous line represents the Standard Model background while the dashed line is the degenerate BESS model expectation.

100 GeV. The number of signal events per year is approximately 2800, the corresponding background consists of 4600 events.

In Fig. 14 we show a case corresponding to $M_{L^\pm} = 1.5 \text{ TeV}$, $g/g'' = 0.1$ and $\Gamma_{L^\pm} = 1 \text{ GeV}$. The following cuts have been applied: $|p_{t\mu}|, |p_{t \text{ miss}}| > 400 \text{ GeV}$ and $E_{\text{miss}} > 200 \text{ GeV}$. The number of signal events per year is approximately 850, the corresponding background consists of 1500 events. The statistical significance of the signal is $S/\sqrt{B} = 22$.

Notice that, the reconstruction of resonance mass, requires a careful study of the experimental setup, due to the smallness of the resonance width.

In this preliminary study we did not consider the production and decay of the corresponding neutral resonances of the model.

16 Conclusions

We have discussed an effective theory describing new vector and axial vector resonances within the scheme of a strong electroweak breaking sector. We have shown that the model has a symmetry which is larger than the one requested by construction. No Higgs particles are required in this effective theory, and moreover the enlarged symmetry guarantees that even with a relatively low energy strong electroweak resonant sector, the severe constraints coming from experimental data, in particular from LEP, are respected.

The new vector and axial vector particles are degenerate in mass (at the leading order) and their virtual effects are suppressed. In the low energy limit ($M \rightarrow \infty$ with the gauge coupling of the new resonances fixed) the new particles are decoupled due to the extended symmetry $[SU(2) \otimes SU(2)]^3$ and we classically obtain the effective lagrangian of the standard model. If we parameterize the deviations from the SM at low energy in

terms of the ϵ parameters, we obtain a deviation from the standard model values only in the next-to-leading order, with a double suppression factor M_Z^2/M^2 and $(g/g'')^2$.

A well known feature of the usual strong interacting models is the relevance of the WW final state. Our model is in this respect different, as the WW final state is on the same footing with the fermionic final state. The reason is that the longitudinal parts of the W 's, related via the equivalence theorem to the absorbed Goldstone bosons, are decoupled from the new resonances. This is due to the absence of coupling between U and L, R (see sect. 2).

For what concerns virtual effects of the new resonances, the model has almost no deviations at low energy with respect to the SM. The situation is completely different if the direct production of the new resonances is considered. This will be possible with the next generation of colliders.

In the case of e^+e^- colliders, LEP2 will not improve the existing bounds from LEP and Tevatron. A substantial improvement can be obtained from higher energy electron-positron colliders, even without considering polarized beams. The most stringent bounds come from cross-section measurements, while asymmetries are less restrictive due to compensations between the two neutral resonances.

High energy hadron colliders, as LHC, will allow to study also the new charged resonances. If the new particles are not discovered, stringent bounds on the model can be imposed by the study of cross-sections as $pp \rightarrow \ell\nu$, in a way similar to the one in which bounds are searched for at Tevatron. The direct observation of the new resonances is possible in a wide window of the parameter space of the model, up to the TeV range, in some case with a spectacular number of events over the background.

References

- [1] S.Coleman, J.Wess and B.Zumino, Phys. Rev. **177** (1969) 2239; C.G.Callan, S.Coleman, J.Wess and B.Zumino, Phys. Rev. **177** (1969) 2247
- [2] M.Bando, T.Kugo and K.Yamawaki, Phys. Rep. 164 (1988) 217
- [3] A.P.Balachandran, A.Stern and G.Trahern, Phys. Rev **D19** (1979) 2416
- [4] R.Casalbuoni, S.De Curtis, D.Dominici, F.Feruglio and R.Gatto, Int. Jour. Mod. Phys. **A4** (1989) 1065
- [5] H.Georgi, Nucl. Phys. **B331** (1990) 311
- [6] R.Casalbuoni, A.Deandrea, S.De Curtis, D.Dominici, F.Feruglio, R.Gatto and M.Grazzini, Phys. Lett. **B349** (1995) 533
- [7] R.Casalbuoni, S.De Curtis, D.Dominici and R.Gatto, Phys. Lett. **B155** (1985) 95; Nucl. Phys. **B282** (1987) 235
- [8] L.Anichini, R.Casalbuoni and S.De Curtis, Phys. Lett. **B348** (1995) 521
- [9] R.Casalbuoni, A.Deandrea, S.De Curtis, N.Di Bartolomeo, D.Dominici, F.Feruglio and R.Gatto, Nucl. Phys. **B409** (1993) 257

- [10] G.Altarelli and R.Barbieri, Phys. Lett. **B253** (1991) 161;
G.Altarelli, R.Barbieri and S.Jadach, Nucl. Phys. **B369** (1992) 3;
G.Altarelli, R.Barbieri and F.Caravaglios, Nucl. Phys. **B405** (1993) 3
- [11] R.Barbieri, F.Caravaglios and M.Frigeni, Phys. Lett. **B279** (1992) 169
- [12] T.Inami, C.S.Lim and A.Yamada, Mod. Phys. Lett. **A7** (1992) 2789
- [13] F.Caravaglios, talk at the EPS conference on Particle Physics, Bruxelles, July 1995
- [14] K.Hagiwara, R.D.Peccei and D.Zeppenfeld, Nucl. Phys. **B282** (1987) 253
- [15] R.Casalbuoni, P.Chiappetta, A. Deandrea, S.De Curtis, D.Dominici, F.Feruglio and R.Gatto, Z. für Physik **C60** (1993) 315
- [16] J.M.Cornwall, D.N.Levine and G.Tiktopoulos, Phys. Rev. **D10** (1974) 1145;
C.G.Vayonakis, Lett. Nuovo Cimento **17** (1976) 17;
M.S.Chanowitz and M.K.Gaillard, Nucl. Phys. **B261** (1985) 379;
G.J.Gounaris, R.Kögerler and H.Neufeld, Phys. Rev. **D 34** (1986) 3257
- [17] F.Abe et al., Phys. Rev. Lett. **74**, 2900 (1995)
- [18] K. Fujii, talk presented at 2nd KEK Topical Conf. on e^+e^- Collision Physics, Tsukuba, Japan, Nov 26 - 29, 1991; published in KEK e^+e^- 1991, 469-502
- [19] J. Layssac, G. Moulataka and F.M. Renard, Int. J. Mod. Phys. **A8** (1993) 3285
- [20] P.Chiappetta and F.Feruglio, Phys. Lett. **B213** (1988) 95
- [21] *Large Hadron Collider Workshop*, Proceedings of the Workshop, edited by G.Jarlskog and D.Rein, CERN 90-10, ECFA 90-133, 1990
- [22] T.Sjostrand, Comp. Phys. Comm. **82**, (1994) 74